2012

Electronic and Structural Properties of Silicene and Graphene Layered Structures

Patrick B. Benasutti
Wright State University

Electronic and Structural Properties of Silicene and Graphene Layered Structures

A thesis submitted in partial fulfillment
of the requirements for the degree of
Master of Science

by

Patrick B. Benasutti
B.S.C.E. and B.S., Case Western Reserve and Wheeling Jesuit, 2009

2012
Wright State University

Wright State University
SCHOOL OF GRADUATE STUDIES

August 31, 2012

I HEREBY RECOMMEND THAT THE THESIS PREPARED UNDER MY SUPERVISION BY Patrick B. Benasutti ENTITLED Electronic and Structural Properties of Silicene and Graphene Layered Structures BE ACCEPTED IN PARTIAL FULFILLMENT OF THE REQUIREMENTS FOR THE DEGREE OF Master of Science in Physics.

Dr. Lok C. Lew Yan Voon
Thesis Director

Dr. Douglas Petkie
Department Chair

Committee on
Final Examination

Dr. Lok C. Lew Yan Voon

Dr. Brent Foy

Dr. Gregory Kozlowski

Dr. Andrew Hsu, Ph.D., MD
Dean, Graduate School

ABSTRACT

Benasutti, Patrick. M.S. Physics, Physics Department, Wright State University, 2012. *Electronic and Structural Properties of Silicene and Graphene Layered Structures.*

Graphene is a two-dimensional nanomaterial with useful and novel properties, but it is a material that does not integrate well with the current silicon microchip infrastructure. Silicene could solve this problem, as it is made of silicon yet retains the novel properties that make graphene desirable. This thesis will outline density functional calculations of a newly proposed structure involving the combination of these two materials. The structure includes silicene layered on graphene in such a manner that it composes a superlattice. It will be examined using the ab-initio density functional theory software Quantum Espresso. This superlattice structure is proposed to have an increase in electronic transport as well as higher binding energy versus standard graphene. Examination of the proposed superlattice is accomplished by using PBE-GGA functionals versus a previous LDA methodology. In conclusion, the results confirm the pattern of increased binding energy in the superlattice as well as increased electron transport, but the amount of increase in the electron transport is not the same as the accepted results. The desirable structural effects of graphene are maintained by the data.

Contents

List of Figures

List of Tables

Acknowledgment

I would like to take this opportunity to extend my thanks to Dr. Lok who, when I switched advisors, offered me guidance and direction. To Dr. Farlow and Dr. Deibel for all their excellent teaching and support. To Dr. Kozlowski and Dr. Patnaik for the teaching and feedback. Dr. Clark for his help with a particularly tough project and Stephen Wynne in CATS for his help with the Linux server. Finally, I would like to thank Dr. Foy for being on my committee at a last minutes notice.

Dedicated to my very recent fiancée who does not care for physics, but puts up with me anyways.

Introduction

A standard computer processor works through the use of silicon based transistors. A transistor can be used for various purposes, such as amplification, logic, and memory. All of these utilities are dependent on the physical properties of the material used to create the transistor. The current rapid advancement in the field of electronics is largely dependent on advances in transistor technology. However, recently transistor technology has reached a plateau. The current methodology is centered about placing more transistors in the same unit area. Through this method the speed and throughput of processors have continued to rise. The speed and efficiency of the processor has changed as well, but if you could dramatically improve the switching speed of a transistor, you could theoretically increase the speed of a processor by an equivalent amount. This thesis will examine a new material that could vastly increase the speed of a transistor. That material is silicene, which is the silicon version of the well-know material, graphene. The method used will be density functional theory implemented through the software suite Quantum Espresso.

Graphene is a two-dimensional version of graphite, and it is has novel properties with respect to its electron dispersion characteristics. The corner of the Brillouin zone in graphene has been shown to exhibit linear dispersion characteristics. This means that fermion charge carriers in this region have an effective mass close to zero. These massless fermions could correspond to unique physical properties, such as increased mobility. However, graphene is composed of a lattice of carbon. This makes it difficult to integrate graphene with current circuitry infrastructures, which are composed primarily of silicon.

Recently, silicene, a silicon version of graphene, has been proposed as a solution to this problem. [1] Silicene is a two-dimensional buckled lattice of silicon atoms with hexagonal lattice structure. A structure of one layer of silicene upon one layer of graphene will be discussed in this thesis. Once again, this proposed structure could be used to bridge the gap between graphene and the bulk silicon infrastructure.

When examining a new material for an application, it is a worthwhile task to use ab-initio calculations to determine the physical properties for that material before investing time and money on manufacture. To that effect the structural and electronic properties of the new structure will be simulated. This simulation will be done using the Quantum Espresso software suite. Quantum Espresso is based on density functional theory, or DFT. Density functional theory relies on many-body theory, among other approximations, to set up the Schrödinger wave equation, abbreviated as SWE. This many-body version of the SWE uses numerous Kohn-Sham equations; they provide the wavefunction of an electron inside a solid. The Kohn-Sham equations are not solvable analytically. They can, however, be solved by approximation methods using Quantum Espresso.

The overarching goal of this paper is to verify the results in a paper by Yong Zhang et al. [2] In the paper there are two conclusions. A superlattice structure is proposed. That structure is a lattice of materials where alternating layers are made of graphene and silicene respectively. Between two layers of graphene there is always a layer of silicene. The silicene is often referred to as an intercalate. From this structure the binding energy of the material is said to increase as well as an increased electron transport in the graphene. This superlattice structure may have the benefit of bridging the gap between graphene and the silicon architecture while adding increased properties over standard graphene or graphite.

Background

Solid state physics is the largest branch of condensed matter physics. It describes various large-scale properties and how they are determined from the atoms and structures of the crystals and or solids in question. Solid state physics, like any field, has many new topics to consider. One of the most often considered new materials in the field is graphene. Graphene is a two-dimensional carbon crystal that has the same structure as a single layer of graphite. Graphene has shown various unique properties that have drawn the attention of the solid state physics community. However it is silicene and the possible integration of silicene and graphene that is the focus of this thesis.

Silicene is a relatively new material, one with a wealth of new topics and possible research. One major reason why silicon nanostructures are of interest is that they may be a viable substitute for graphene. Again, graphene is a two-dimensional lattice of carbon atoms with hexagonal structure. Graphene has shown characteristics that make it desirable in theoretical as well as practical applications. The band structure of graphene shows similar characteristics to the solution to a version of the Dirac equation, notably the version that describes massless fermions. As was mentioned this characteristic may lead to graphene having a much larger electron mobility than many current devices. [3] However graphene does not integrate well with the current infrastructure, which is silicon based. This thesis will focus on how silicene may be helpful in this regard. It has been theorized that silicene has the same beneficial properties as graphene. Various structures have been proposed to integrate the two materials. [2] Bilayer graphene and silicene will be used as a model for the

more complicated structure, called a superlattice. However, before that is done the general structures of both graphene and silicene will need to be outlined.

2.1 Structure

The first thing to consider in a crystal structure is the lattice type and then the unit cell. The basic lattice type of graphene is hexagonal and the unit cell placed at each lattice point has two atoms. In Figure 2.1, the light colored atoms labeled one through four, are the atoms located at lattice points of the hexagonal structure. The darker-colored atoms, for example atom number 5, are the second atom in the unit cell. Here the distinctive hexagons that make up graphene are outlined. [3] The next physical property that needs to be verified are the lattice parameters of the two materials. The parameters of silicene have been determined by density functional theory as well as by experimental methods, prior to this paper. One of the most often cited papers for the parameters of silicene determined by computational methods gives the lattice parameter of silicene to be 3.89 $\mathring{A}$. [4] From that lattice parameter, the minimum bond length oof 2.25 $\mathring{A}$ can be determined. The lattice parameter of graphene is also well known and is approximately 2.45 $\mathring{A}$. [5] Figure 2.1 outlines the general structure for both graphene and silicene, however silicene has a pseudo two-dimensional structure. In silicene the darker colored atoms, have a buckling in the z-direction. Where a buckling is when the second atom in the unit cell is depressed from the flat plane of the lattice so that the structure is no longer purely two-dimensional.

The lattice vectors of the hexagonal lattice with respect to the frame of reference used in the software Quantum Espresso are as follows:

$$\vec{a_1} = a\,\hat{i}, \tag{2.1}$$

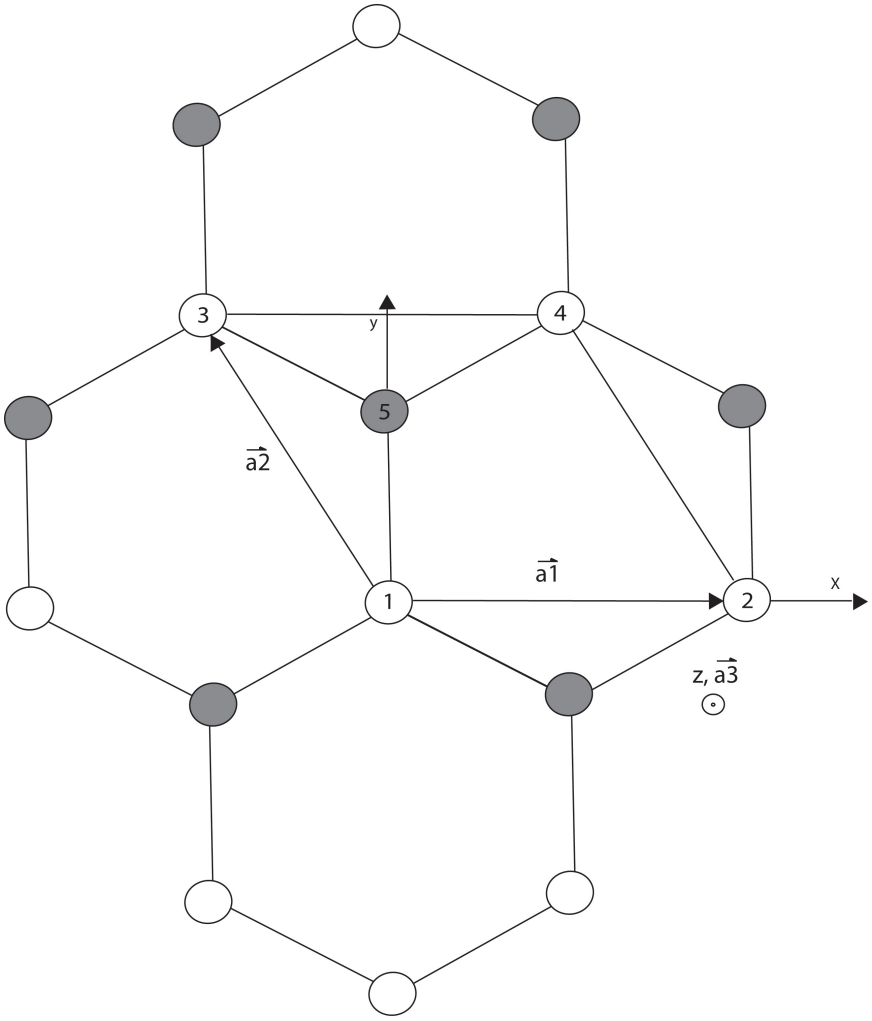

Figure 2.1: Silicene

$$\vec{a_2} = -\frac{a}{2}\,\hat{i} + \frac{\sqrt{3}a}{2}\,\hat{j}, \tag{2.2}$$

$$\vec{a_3} = \hat{k}. \tag{2.3}$$

The next parameter to examine is the buckling amount of the second atom in the unit cell. The distance of this buckling parameter (Δz) is often given as 0.44 $\mathring{A}$. [6] While silicene may seem three-dimensional due to the buckling parameter, it is more like a pseudo two-dimensional structure. The structure is actually two-dimensional except for that buckling parameter. Keep in mind that the vector a_3 is only present for calculation reasons in the case of the two-dimensional structures. The buckling amount will be verified in the calculations section. Notice the buckling amount will vary when introduced into the bilayer and superlattice structure. But the buckling amount of stand-alone silicene will be verified so that Quantum Espresso can be proven effective.

2.1.1 Band Structure

Once the lattice structure is determined, the next step is to determine the band diagrams of these silicene-graphene composites. To accomplish that one needs to construct the Brillouin zone of this hexagonal lattice. Using the Wigner-Seitz construction method to build the Brillouin zone in reciprocal space, the Figure 2.2 is drawn using equations 2.1 through 2.9.

The Brillouin zone has some symmetry points that will be used to plot the band structure. The equations for the reciprocal vectors as well as the equations for the points in the Brillouin zone used to plot the band structure are,

$$\vec{b_1} = \frac{2\pi}{a\sqrt{3}}\left(\sqrt{3}\hat{k_x} + \hat{k_y}\right), \tag{2.4}$$

$$\vec{b_2} = \frac{4\pi}{a\sqrt{3}}\,\hat{k_y}, \tag{2.5}$$

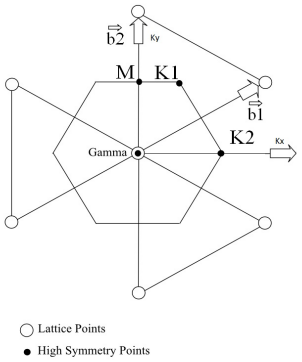

Figure 2.2: The Brillouin zone of silicene

$$\vec{b_3} = 2\pi\ \hat{k_z}. \tag{2.6}$$

Which are derived from the equations,

$$\vec{b_1} = 2\pi \frac{\vec{a_2} \times \vec{a_3}}{\vec{a_1} \cdot [\vec{a_2} \times \vec{a_3}]}, \tag{2.7}$$

$$\vec{b_2} = 2\pi \frac{\vec{a_3} \times \vec{a_1}}{\vec{a_1} \cdot [\vec{a_2} \times \vec{a_3}]}, \tag{2.8}$$

$$\vec{b_3} = 2\pi \frac{\vec{a_1} \times \vec{a_2}}{\vec{a_1} \cdot [\vec{a_2} \times \vec{a_3}]}. \tag{2.9}$$

Any vector in the reciprocal space can be written in terms of the cartesian coordinates, which is how the equations 2.10 through 2.12 can be derived. The high symmetry points in the Brillouin zone will be written in this frame of reference. The units of $\frac{2\pi}{a}$ are pulled out to the front. Keep in mind, that in equation 2.6, because the lattice is purely two-dimensional the lattice parameter cancels out of the equation.

$$\vec{\Gamma} = \frac{2\pi}{a}\,[0, 0, 0] \tag{2.10}$$

$$\vec{M} = \frac{2\pi}{a}\left[0, \frac{1}{\sqrt{3}}, 0\right] \tag{2.11}$$

$$\vec{K} = \frac{2\pi}{a}\left[\frac{2}{3}, 0, 0\right] \tag{2.12}$$

Knowing this information it is possible to graph the band structure of the material between these points. It is important to note that the Brillouin zone of the two materials will be the same.This produces two sets of coordinates that are used for the graphing of the Brillouin zone to be very similar, if not identical. The actual calculations and results will be outlined more thoroughly in the Data and Calculations sections.

2.2 External Research

This section will cover some of the recent research in the field of silicene simulations. Simulation is a valuable tool used to determine the properties of a material and has been widely used to characterize silicene. A semi-exhaustive list of all the research to date in this field will be covered herein. A simulation method often used to determine the electronic and physical structures of silicene is density functional theory. Density functional theory has some major pros and cons, as it is very capable at determining the structure of a system, but it is not as capable at determining the energy band structure. [7] There are various types of software that have been used for this kind of calculation, and all of them rely on density functional theory. Various papers have been published on this topic. Of those there have been several Siesta software calculations, [8–12] some with the Vienna software. [13–17] ABINIT and CASTEP were also used. [18, 19] This is not a complete list of the software's used but it provides a good coverage of the types of software used. The software that will be used for this project is called Quantum Espresso. There have been various papers using this software on similar topics. [12, 4, 20, 21]

2.3 Physical Parameter Verification

As silicene is proposed substitute for graphene one will want to make sure to understand the electronic and structural parameters of the material. Graphene is known to have a lattice parameter of $2.45\mathring{A}$. [5] The knowledge of the parameters will be of particular use when building simulations of graphene. It is also shown that silicene has a comparable electronic structure to graphene. Notably, the often talked about Dirac points appear to be present in silicene. These Dirac points give rise to the massless Dirac fermions which have caused a large amount of interest in graphene. Their presence in silicene continues to establish the motivation for research in silicene. [9] The theoretical foundation of silicene's structure has been well established by computational methods in previous sections. In order to determine the suitability and usefulness of the material experiments needed to be performed. There were a variety of experiments done to verify the parameters of silicene. The first and most prominent method used to determine the parameters is a method called angle resolved photoelectron spectroscopy or ARPES. ARPES is useful because it is one of the most direct methods of determining the electronic structure of materials. [22] These parameters are often determined while the silicene is on a silver substrate. Silver has a similar structure to that of silicene leading to easy deposition. Another prominent methodology is called scanning tunneling microscopy. Scanning tunneling microscopy or STM creates an image of the surface and from those images it is possible to directly view the structure of the nanosheets. From STM analysis there are indications that silicene forms a buckled structure. This structure can be identified because the first atom in the unit cell is raised above the second atom in the same cell. [23] Graphene is known to have a standard honeycomb structure where the second atom is not displaced out of the plane, but remains in a flat two dimensional structure. [24]

2.4 Future Research

Now that it has been determined that future research in silicene is worth investigation, the focus of the articles reviewed will be narrowed tol provide more focus on the topic. The articles that are of particular interest to the future research of this project are ones that outline silicene deposited on a substrate. Silver and aluminum nitride are the two types of substrates proposed for silicene. The growth of silicene on silver has been definitively demonstrated. The creation of silicene on silver is a multi-step process involving high vacuum evaporation. [25–27] Another topic that is of interest and has already been researched is the effect of hydrogenation on silicene. Silicene is not magnetic under normal circumstances, however the hydrogenation of silicene can introduce magnetism as well as a significant shift in the electronic properties. [28] The adsorption of various elements on silicene is useful to study as it illuminates the effectiveness of hydrogenation of silicene as determined by Quantum Espresso. There is some speculation that adsorption may have other uses such as expanding the band gap of the two materials in question. [29] The storage of hydrogen is another way that hydrogenation can be useful. Energy or hydrogen storage is a research topic that is highly in demand. A good method to store hydrogen is in high demand and is a valuable research possibility. As fossil fuels become more and more scarce the search for renewable energy will continue to grow. The possibility of silicene as a hydrogen storage structure has already been researched. [30]

The optical properties of silicene are also of merit. Silicene could theoretically be used in solar cell applications as well as various optical detection circuits. As was mentioned before, renewable energy sources are viable and lucrative research topics that may need continuing research. Silicene's optical properties were investigated using density functional theory and were considered feasible for future research. This article outlines this feasibility and paved the way for more research in the area of silicene photodiodes. [9]

To delve more into relevant topics, we want to examine papers on multiple layers of silicene. This will hopefully provide insight into the bilayer and superlattice proposed

structures this paper covers. Silicene as a two-dimensional sheet has been researched in a definitive manner, but silicene in combination with other materials is still full of potential. A cursory search does not reveal any papers that immediately overlap with the proposed research, which is promising, since this paper hopes to provide new insights. There has been some research into multiple layers of silicene and the friction between them. [31] One of the challenges when dealing with placing another material on top of another is called reconstruction; it is when the material in question changes from its crystal structure, at the interface with another material, to accommodate the differences between the two. Some insight may be garnered from an article detailing the molecular dynamics between two different sheets of silicon. [32]

2.5 Density Functional Theory

Density Functional Theory is one approximate solution to the many-body theory of solids. Many-body theory is well known to be unsolvable analytically, so an approximation must be made. There are various approximations and computational methods that are used to give a good approximation to the solution of this problem. They are discussed herein.

2.6 Many-Body Theory

2.6.1 Born-Oppenheimer Approximation

There are many approximations that one must make when dealing with a many-body problem in the realm of solids. The first one is known as the Born- Oppenheimer approximation. This approximation is based on the idea that in a solid the nuclei are not moving as quickly as the electrons. The nuclei, which are approximated as ions in this case, are assumed to be stationary. Since the electrons are much less massive and move at much higher velocities

than the nuclei, the positions of the electrons are considered variables and the positions of the ions are considered parameters. In order to examine this situation we define the general Hamiltonian for a many-body system from the standard Hamiltonian. Remember the basic Hamiltonian in this situation is the potential and the kinetic energy as in,

$$H = T + V \quad where \quad T = \frac{-\hbar^2}{2m}\nabla^2. \tag{2.13}$$

However the potential, V, changes based on the potential of the system. There are two kinetic energy terms and three potential energy terms that needed to be added. They can be written as,

$$H = \frac{-\hbar^2}{2m}\sum_{e}^{n}\nabla_i^2 - \frac{-\hbar^2}{2m}\sum_{i}^{n}\nabla_i^2 - \sum_{i,e}^{n}\frac{Z_i e^2}{4\pi\epsilon_0 r_{ei}} + \frac{1}{2}\sum_{i,j}^{n\prime}\frac{Z_i Z_j e^2}{4\pi\epsilon_0 r_{i,j}} + \frac{1}{2}\sum_{e,e}^{n\prime}\frac{e^2}{4\pi\epsilon_0 r_{ee}}. \tag{2.14}$$

Where the subscripts (i,j) refer to ions and the subscript (e) refers to the electrons. The key components of the mathematical Born-Oppenheimer approximation are that first the nuclear energy term is left separate and that the positions of the electrons with respect to the ions in the nucleus are considered as parameters. Essentially the fourth term is neglected and the term r_{ei} is changed into a set parameter. This allows a great simplification of the equations when dealing with solids.

2.6.2 Hartree Energy

The Born-Oppenheimer approximation begins the outline a many-body Hamiltonian in a useful manner by reducing out various terms. But the many-body problem is a complex one and the Hamiltonian derived in the Born-Oppenheimer is still not suitable for calculations. There are further approximations that must be made to achieve better accuracy and

minimize calculation time. That is what is involved in the derivation of the Hatree Energy equations.

As was mentioned previously the Schrödinger wave equation will be used to solve for the energy of the many-body solid. First, take the Hamiltonian that is defined in the Born-Oppenheimer approximation and put it into the SWE with a new wavefunction. Then to define a wavefunction as a new combination of products of the wavefunctions that correspond to individual electrons. It can be written as,

$$\Psi = \phi_1(r_1)\phi_2(r_2)\phi_3(r_3)\ldots\phi_n(r_n). \tag{2.15}$$

However this wavefunction cannot be put straight into the Schrödinger wave equation without some analysis and manipulation. The first step is to use the variational principle to analyze and set the energy of a system involving these wavefunctions. Our overall goal is to find the ground state and the variational principle places a limit on the minimum energy of the system. It outlines the equation below, where the ϵ is defined as,

$$E = \frac{\langle\Psi|H|\Psi\rangle}{\langle\Psi|\Psi\rangle}. \tag{2.16}$$

Where $E \geq E_0$ and E_0 is the ground state energy of the system. From this it is possible to get an energy minimum. However that minimum is not necessarily the ground state energy. This method

Using this variational principle one can derive the Hartree energy equation Using these equations and the variational principle it is possible to derive the Hartree Energy equations, however it more useful to include the Pauli-Exclusion principle and show the Hartree-Fock equation as the equations are essentially the same.

2.6.3 Hartree Fock Theory

The Hartree energy equations can be useful under some specific circumstances, but they still lack some important characteristics. Primarily, the lack of spin is troubling. It can be included in a post analysis. However, that is an ad-hoc solution and doesn't contain useful information. spin characteristics into the wavefunction from the beginning. It can be done by using what is called the Slater determinant. The Slater determinant,

$$\Psi(x_1 \dots x_n) = \frac{1}{\sqrt{n!}} \begin{vmatrix} \Phi_1(x_1) & \Phi_2(x_1) & \dots & \Phi_n(x_1) \\ \Phi_1(x_2) & \Phi_2(x_2) & \dots & \Phi_n(x_2) \\ \dots & \dots & \dots & \dots \\ \Phi_n(x_n) & \Phi_n(x_n) & \dots & \Phi_n(x_n) \end{vmatrix} . \tag{2.17}$$

A slater determinant, as in above is an n by n matrix that includes the Pauli exclusion principle, which is essential if each state has to be unique. If $\phi_i = \phi_j$ then two columns of the determinant would be 0. This is desirable as makes sure that a non-physical situation such as the equality of two different states cannot happen.

It can be written in a more straightforward fashion with a permutation operator such that,

$$\Psi(x_1 \dots x_n) = \frac{1}{\sqrt{n!}} \sum_p (-)^p P \left(\Phi_1(x_1)\Phi_2(x_2) \dots \Phi_n(x_n)\right) . \tag{2.18}$$

This permutation operator works by switching either the coordinates or the subscripts of the Φ wavefunctions. Keep in mind that these individual wavefunctions are orthogonal in a manner such that,

$$\langle \Psi_i(r_k) | \Psi_j(r_k) \rangle = \delta_{ij} \tag{2.19}$$

is true. Using this information and methodology it is possible to derive the Hartre-Fock

Equations, which boil down to,

$$\left(-\frac{\hbar^2}{2m} + V(r) + V_H(r) + \right)\phi_i(r) = E_i\phi_i(r) \tag{2.20}$$

Where the $V_H(r)$ term is the Coulomb repulstion term which can be written as,

$$V_H(r) = e^2 \int \frac{n(r^{'})}{|r - r^{'}|} d^3r^{'}. \tag{2.21}$$

These equations are useful but still lack an approximation for the exchange correlation potential, which is covered in a later section.

2.6.4 Density Functional Theory

Now that the fundamentals of the Hartree-Fock and the Hartree energy equations have been reviewed, there is a system of equations that covers the many-body problem between the electrons and the ions in a solid. The equations that have been derived are correct, but have a large number of variables and are therefore not useful. For example the wavefunction of each electron in a solid would need to be solved and a solid of any significant volume would have a number of electrons on the order of Avogadro's number. This is an impractical number of equations to solve; so in order to find a useable solution one needs to find a way to condense these equations.

Hohenberg, Kohn and Sham together developed a method to deal with the many-body problem. This approach involves a method that relies on electron functionals. The theorem dictates that a potential can be determined uniquely from the ground state electron density. It also goes on to say that the reverse is true. From a known potential one can determine the electron density. One knows this because a definite electron potential fixes the Hamiltonian. Which is known from the existence theorem. The existence theorem states that a density functional uniquely determines the Hamiltonian.

The software uses density functional theory as the basis of the solutions. So a functional needs to be defined. A functional takes a function and defines a single number from the function, such as,

$$F[f] = \int_{-1}^{1} f(\mathbf{x})\mathbf{dx}. \tag{2.22}$$

So the Hohenberg and Kohn's theorem is such that a ground state energy can be expressed as $E[n(r)]$ where $n(r)$ is the electron density and hence the reason for the name density functional theory. [33]

That means that one needs to come up with an expression for $n(r)$. This is where the Thomas-Fermi contribution to the theory needs to be outlined, which will illuminate further practical steps. Thomas and Fermi posited that the electron density is uniquely determined by the potential. To start, one need to know the density of states as in,

$$N = V \sum_{\sigma} d\mathbf{k}\rho(\mathbf{k}) = \frac{\mathbf{2}}{(\mathbf{2}\pi)^{\mathbf{3}}} \frac{\mathbf{4}\pi}{\mathbf{2}\pi} \mathbf{k_f^3 V}. \tag{2.23}$$

This is a well-known equation. It outlines the the amount of energy states that electrons can occupy in a given volume. When one know the density of states one can estimate the kinetic energy of particles in the system. From the kinetic energy it is possible to estimate the potential. However this estimation is not complete, for example there is something called exchange correlation energy that is not included, and that leads to large systematic errors in the final answers. The exchange correlation energy is actually two terms that have been combined into one energy. Both energies are unknown in the current formalism and must be approximated, so to simplify matters they have been combined.

An exchange energy refers to the exchange interaction theory. In that theory, particles with overlapping wavefunctions of identical particles have different energies than expected. The correlation energy is often referred to as the Coulomb correlation and has to do with the the coulombic repulsion spatial characteristics of atoms. One of the primary goals of den-

sity functional theory is to come up with a good approximation of the exchange-correlation energy, which will be discussed more in the Local Density Approximation section.

2.7 Kohn Sham Equations

The Kohn-Sham equations are often broken down into three equations that give essentially the same information as the Hartree and Hartree-Fock equations. However this new equation is a single equation versus the many-body equations in the previous versions. Keep in mind that these two methods are not equivalent. The Kohn-Sham enable a mapping of the original Hartree-Fock equations that can yield a similar answer. Which is the ground state electron density of of the system. Density functional theory is only capable of determining the ground state density of the system. If an excited state is desired it is possible to figure that out from the ground state.

Next the Kohn-Sham equations need to be derived. Fortunately, however, the procedure to derive them is very similar to the process shown in the derivation of the Hartree and Hartree-Fock methods. It involves the variational principle and minimizing the expectation value of the Hamiltonian. For the sake of the reader only the solution and salient points will be given. For details on the derivation one can see Patterson and Bailey's Solid-State Physics: Introduction to the Theory, a large amount of the theory is was garnered from this source [34] as well as private lectures with Dr. Lok C. Lew Yan Voon. [35] The Kohn-Sham equations end up giving a set of equations similar to the Euler-Lagrange equations seen in classical mechanics. However the variable that would normally be used in the Euler-Lagrange is replaced by a wavefuction. It can be seen through the variational method that these equations based on the new functional definition of the energy start as,

$$F[n] = F_{KE}[n] + E_{xc}[n] + \frac{e^2}{2}\int \frac{n(r)n(r^{'})d\tau d\tau^{'}}{|r - r^{'}|}. \tag{2.24}$$

Knowing this one can then obtain the Euler-Lagrange equations for this system as

$$\frac{\delta F_{KE}[n]}{\delta n(r)} + v_{eff}(r) = \mu. \tag{2.25}$$

Which when one substitutes in,

$$n(r) = \sum_{j=1}^{N} |\phi_j(r)|^2 \tag{2.26}$$

as the electron density, we can then obtain one form of the Kohn-Sham Equation as,

$$\left(-\frac{1}{2}\nabla^2 + \nu_{eff}(r) - \epsilon_j.\right)\phi_j(r) = 0. \tag{2.27}$$

2.8 Local Density Approximation

There is a crucial last local density approximation that needs to be mentioned. This approximation can help to actually calculate the electron density as if it were a uniform electron gas with the density of states as mentioned above. Over a small enough region one can always make this approximation. From a summation over all the regions it is possible to get an approximate expression for the entire solid. So first one wants to write down an effective potential such that,

$$\nu_{eff}(r) = \nu(r) + \int \frac{n(r^{'})}{|r - r^{'}|} dr^{'} + \nu_{xc}(r). \tag{2.28}$$

This is the same effective potential as before. The next step is to write down a new exchange correlation energy for this approximation which can be written as

$$E_{xc}^{LDA} = \int n e_{xc}^{u}[n(r)]dr. \tag{2.29}$$

Keep in mind that this exchange energy is representative of the energy for each particle. This new energy can be rewritten as, $\nu_{xc}(r)$ as

$$\nu_{xc}(r) = \frac{\delta E_{xc}[n]}{\delta n(r)}. \tag{2.30}$$

Which is the final theoretical step one needs before moving these equations into practical applications.

2.9 Basic Algorithm

All of the basic theory has been outlined about density functional theory, but theory is not enough. The methodology needs to be outlined so that a more functional understanding of the theory can be obtained. As was mentioned the goal is to obtain the ground state energy of a many-body system. With that goal in mind an algorithm has been outlined in figure 2.3, to defined the method used to solve the Kohn-Sham equations in Quantum Espresso.

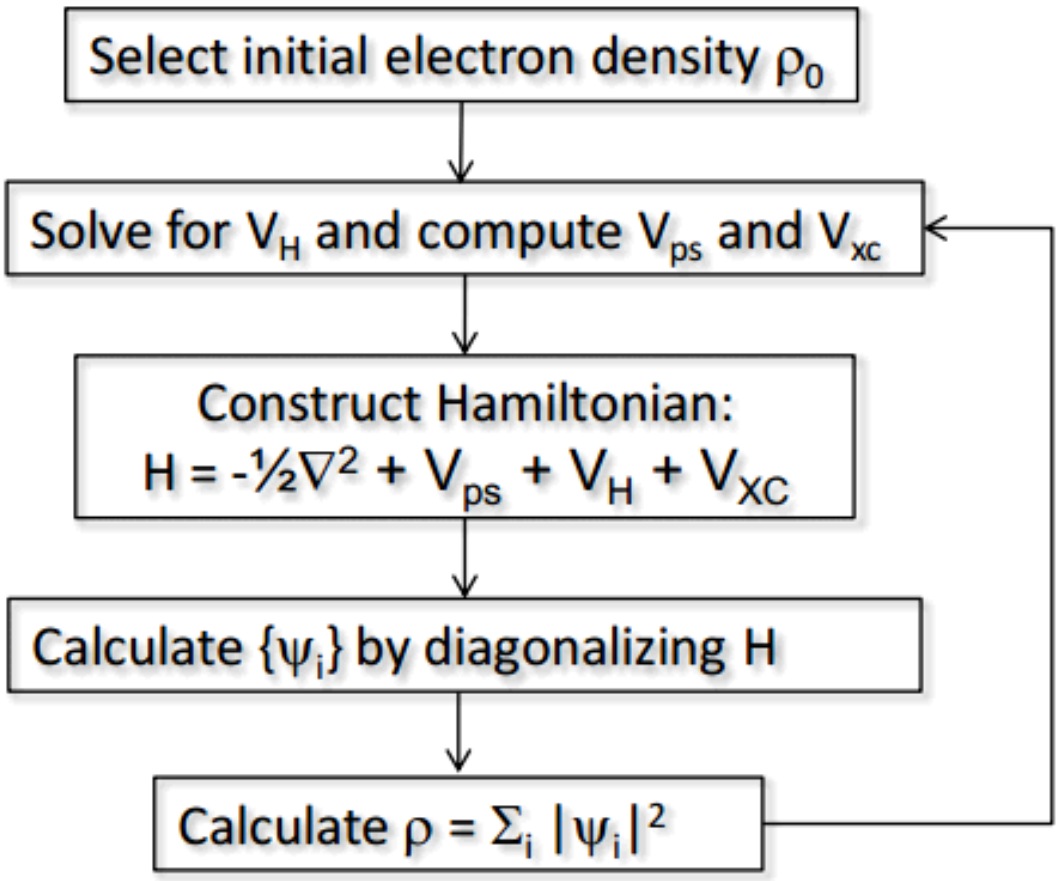

Figure 2.3: A flowchart of a Kohn-Sham equation algorithm [36]

2.10 Research Goals

There are specific data goals that this paper will attempt to verify as well as new research to propose. The data that needs to be verified is first, the increase in binding energy, and secondly the shift of the Fermi energy of the SiC_2 superlattice. The binding energy of the superlattice is supposed to increase with respect to graphite and the Fermi level is supposed

to shift upwards. [2]

The topics that are new to this paper are twofold. First the type of pseudopotential used herein will be a different kind to see if there are any major changes between the old and the new. Secondly the characteristics of a second type of superlattice will be outlined. This new superlattice designated Si_2C_6, will be outlined and examined as a possible useful structure as it has lower symmetry than the SiC_2 structure.

2.11 Binding Energy

One of the key goals of this paper is to show that the interlayer binding energy of the superlattice is better than graphite. In order to verify this it is important to understand how to calculate the interlayer binding energy. The values of the interlayer binding energy of two types of graphite are given as 1 and 2. [2] In order to calculate it for a new material, there are three needed. First, one needs the energy of each type of atom in the lattice. This is done in the software by creating an atom inside a very large unit cell and minimizing the energy. Secondly, one needs the energy of each layer of the structure in question. There are two distinct layers in each superlattice, so the energy of layer will be needed. Finally, one needs the energy of the total superlattice. The binding energy of a lattice such as the one under consideration is calculated through the following formula. $EB = \frac{(Elat - \sum_i (Esingle_i)}{N}$. [2] Where EB is the binding energy, Elat is the energy of the superlattice, and Esingle is the energy of each layer of the lattice and N is the number of atoms in the unit cell.

2.12 Band Structure

The other major goal of this paper is to verify that the Fermi energy of the band structure shifts with respect to the Dirac points of the band structure. The band structure diagram of the superlattice in the data from Zhang, predicts and upward shift of the Fermi level with

respect to the dirac point of the band structure of silicene. This upward shift of the Fermi level corresponds to an increase in the electron transport properties of the graphene. [2] It is this papers goal to reproduce this upward shift shown in Figure 2.4.

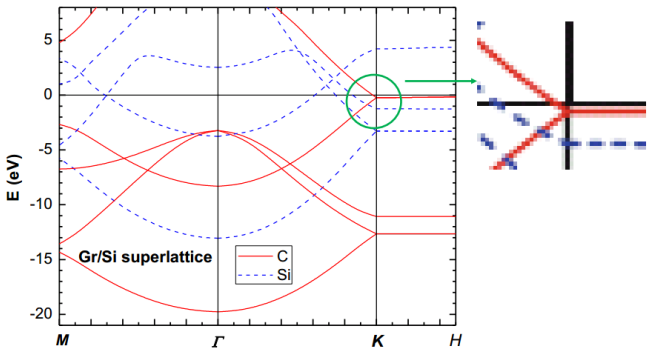

Figure 2.4: SiC_2, bilayer band structure, note the Fermi level position [2]

2.13 PBE-GGA pseudopotentiall

One of the major differences in methodology between the original paper proposed by Zhang et al and this paper, is the difference in the types of functionals used to generate the data. A standard pseudopotential in the previous methodology was generated using the local density approximation for the exchange correlation. The pseudopotentials used in this project were generated using the Perdew-Burke-Ernzerhof Generalized Gradient Approximation to estimate the exchange correlation.

Calculations

3.1 Introduction to Calculations

Now that the background has been outlined the data can be analyzed in a comprehensive manner. The first thing that needs to be covered is how to relate the structures in a manner that the Quantum Espresso software can understand. Often data will be presented as the output of a program; every effort will be made to interpret the output for the reader in an logical manner. Then a verification of the Quantum Espresso will be completed and finally the actual superlattice combination structure will be covered.

In order to use a software package for research, several calculations need to be made in order to verify that the program is working to an acceptable level of accuracy. This is done to a rigorous extent as a major criticism of such methods, is that it is difficult to verify the results that are obtained. Various similar verification calculations serve a dual purpose. They are conducive to the learning of the software and also provide appropriate benchmarks for accuracy.

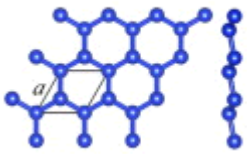

[37]

Figure 3.1: Graphene

3.2 Structural Calculation of Graphene Parameters

The first benchmark that we want to use to verify Quantum Espresso's accuracy is the calculation of the structural parameters of graphene. It was mentioned earlier that silicene may be used to replace graphene in certain applications. Then it is only prudent to make sure that the parameters of graphene, a simpler material, can be calculated first. Below is the input code provided for the graphene calculation.

```
&CONTROL
  calculation ='relax',
  restart_mode='from_scratch',
  pseudo_dir  = "/home/w003pbb/espresso-4.3.2/pseudo",
  outdir      = "/home/w003pbb/tmp",
/
&SYSTEM
  ibrav       = 4,
  celldm(1)   = 4.64117D0,
  celldm(3)   = 12.2149837D0,
  nat         = 2,
  ntyp        = 1,
  ecutwfc     = 60,
  occupations = "smearing",
  smearing = 'fermi-dirac',
  degauss = 0.02,
/
```

```
&ELECTRONS
  conv_thr    = 1.D-8,
  mixing_beta = 0.3D0,
/
&IONS
  ion_dynamics      = "bfgs",
  pot_extrapolation = "atomic",
/
ATOMIC_SPECIES
C   12.0107  C.pbe-van_bm.UPF
ATOMIC_POSITIONS
C   0.0000000      0.0000000     0.000000
C   0.0000000      0.67735027    0.000000


K_POINTS automatic
 30 30 1 1 1 1
```

Each of these input parameters have meanings that need to be considered. Any of the sections that have an ampersand are described in the literature as ”cards” and the rest are simple parameter specifications. Each equality such as $calculation =' relax'$ will be considered a field. The first card is CONTROL and it describes various parameters like bookkeeping for the system. There are two important fields to mention here.

The first is $calculation = 'relax'$, which determines the type of calculation to complete where the various types of calculations are explained in the appendix. In this case the relax calculation uses Newtonian mechanics to minimize the energy of the system from a

purely geometric energy standpoint.

Secondly $restart\_mode = \ 'from\_scratch'$ this field tells the program to restart the calculations from scratch if there is a problem.

The SYSTEM card describes the structure of the system under calculation. The field $ibrav = 4$ tells the type of bravais lattice to use for the calculation, in this case the 4 stands for the hexagonal lattice. The field $celldm(1)$ and $celldm(3)$ give the lattice parameters for a, b and c respectively. The parameter c is only included as the program requires it; it will be given as very large value to separate the layers and provide separation. The $D0$ part is simply an addition that tells the system to use the input without rounding the decimals. The field $nat = 2$ gives the amount of atoms in the unit cell. The field $ntyp = 1$ tells the system how many types of atoms there are in the unit cell. The field $ecutwfc = 30$ gives the energy cutoff for the wavefunction calculations in units of Rybergs. Rydbergs in S.I. units are 13.6 ev. The cutoff energy for the wavefunction tells how much energy can be used for the dispersion relation of the plane-waves used to determine structure of the system. The field $occupations = "smearing"$ tells the system to use the smearing method. The field $smearing = \ 'gauss'$ tells the system the type of distribution to use when smearing. For graphene a gaussian distribution can work to properly determine the structure. However for silicene a fermi-dirac distribution is needed.

The ELECTRONS card has only two key fields. The first field is $conv\_thr = 1.D-7$ which gives the value for the convergence threshold of the energy of the final wavefunctions. The calculations will finish when the value of the self consistent calculation gives an energy difference less than the threshold. The field $mixing\_beta = 0.3D0$ tells the system that when it gets results to feed them back into the calculations with a percent equal to the $mixing\_beta$ parameter.

The IONS card describes different ways to run calculations when dealing with a relaxation calculation. The $ion\_dynamics = "bfgs"$ field tells the system which algorithm to use when dealing with the relaxation. The $pot_extrapolation = "atomic"$ field describes

the type of potential extrapolation to be used.

The first set of parameters, the ATOMIC SPECIES card gives the information to be used by the machine for the atoms in the system. The C part is the abbreviation for carbon and later will be changed to Si for silicon. The next value gives the atomic weight. The final value in this parameter is the name of the pseudopotential file to be used.

The last set of parameters are the K POINTS and these parameters gives various ways to determine the K POINTS used for various calculations like the band structure.

All fields have been explained, except for the ones inside the ATOMIC POSITIONS parameter. It is in units of lattice parameters (alat) which is set to 4.64117. It is converted to Angstroms to make it more palatable. First 4.64117 is converted back to angstroms first as it is in bohrs. It now equals 2.456, which is the accepted value. Graphene B, the second Carbon in the card, is at a y-distance which is multiplied by the lattice parameter to get 1.42 angstroms, the accepted minimum bond length. [3] Keep in mind that 0.577503 in lattice parameters is 1.42 in Angstroms, which is the final value. Now to test that everything is working properly, the Y input parameter of the B carbon was shifted by a factor of 0.1 from the desired and as expected Quantum Espresso corrected the shift back to the desired parameter, which can be seen below.

```
Input parameters

ATOMIC_POSITIONS

C   0.0000000      0.0000000     0.000000

C   0.0000000      0.67735027    0.000000


Output positions.

ATOMIC_POSITIONS (alat)

C         0.000000000   0.049999564   0.000000000
```

```
C         0.000000000   0.627350706   0.000000000
End final coordinates
```

In the final parameters you can see that 0.627350706-0.049999564 = 0.57735027. Which is the minimum bond length parameter returned within an acceptable percentage in units of lattice parameter (a).

3.3 Silicene Structural Parameter Calculations

The second benchmark that will be useful for this program is the calculation of silicene's structural parameters.

```
&CONTROL
  calculation ='vc-relax',
  restart_mode='from_scratch',
  dt          = 30.D0,
  pseudo_dir  = "/home/~",
  outdir      = "/home/~",


/
&SYSTEM
  ibrav       = 4,
  celldm(1)   = 7.35304D0,
  celldm(3)   = 5.132002392D0,
  nat         = 2,
```

```
  ntyp        = 1,
  ecutwfc     = 60,
  occupations = "smearing",
  smearing    = "fermi-dirac",
  degauss     = 0.003D0,
/
&ELECTRONS
  conv_thr    = 1.D-8,
  mixing_beta = 0.3D0,
  diago_david_ndim = 2,


/
&IONS
  ion_dynamics      = "bfgs",
  pot_extrapolation = "none",
  wfc_extrapolation = "none",
/


&CELL
  cell_dynamics = ’bfgs’,


/
ATOMIC_SPECIES
```

```
Si   28.086  Si.vbc.UPF

ATOMIC_POSITIONS (angstroms)

Si   0.0000000      0.0000000     0.000000

Si   0.0000000      2.200000    -0.440000


K_POINTS automatic

  30 30 1 1 1 1
```

Each of these input parameters has been explained , except for the new values in the ATOMIC POSITIONS card. It is in units of angstroms. The three position components of each atom have been given as the three values after each Si label. The output of the silicene file gives upon completion as,

```
     the Fermi energy is    -3.2084 ev


     Final enthalpy =     -15.7511018894 Ry


CELL_PARAMETERS (alat=  7.35304000)
   0.980796776   0.000000000   0.000000000
  -0.490398388   0.849350383  -0.000454249
   0.000000000  -0.002758610   5.124605488


ATOMIC_POSITIONS (angstrom)

Si       0.000000000  -0.021913866   0.000013120
```

```
Si       -0.000000000   2.179790137  -0.440532883

End final coordinates
```

Here one can see that both the coordinates have shifted slightly but are well within what would be considered acceptable errors. Using Pythagoreans theorem one can get the Si-Si bond length of approximately 2.25 $\mathring{A}$, and one can directly determine the appropriate length of the ΔZ which is approximately -0.44 $\mathring{A}$. It is worthwhile to note that the original file gives slightly different values from the accepted so as to show that it is not simply taking in a value and outputting the same. It does indeed converge to the accepted values on its own.

3.4 Band Structure Calculations

The next benchmark, before moving onto the primary calculation, is the calculation of the band structures of both graphene and silicene. The band structure is a visual representation of the energy levels that the electrons can have inside the solid. These calculations are done almost entirely within the Quantum Espresso suite of programs. If the objective is just to complete a band structure calculation, that is accomplished by calculating an integral over the brillouin zone of the crystal. However, Quantum Espresso does the numerical integration in an earlier step so then all that is needed is to designate the points desired for plotting.

The brillouin zone of graphene, and essentially silicene, is a two dimensional hexagon. The band structure and outline of the Brillouin zone is well known. The figure below is the author's depiction of the Brillouin zone. Table 3.1 outlines the coordinates of the key points in the brillouin zone. Keep in mind that the table outlines the coordinates in multiples of

u, v, w from equation 2.7.

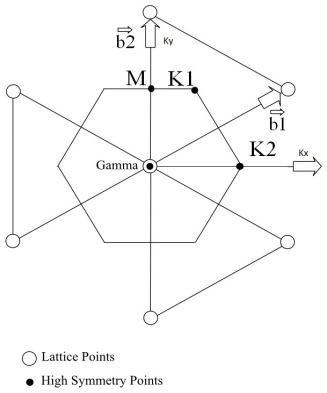

Figure 3.2: The Brillouin zone of silicene

Table 3.1: Brillouin Zone Coordinates Table

Coordinates	x	y	z
Γ :	0	0	0
M:	0	$\frac{1}{\sqrt{3}}$	0
K1:	$\frac{1}{3}$	$\frac{1}{\sqrt{3}}$	0
K2:	$\frac{2}{3}$	0	0

Once again Quantum Espresso uses density functional theory to calculate the band structure using the Kohn-Sham equations, however it is well known that the band structure has significant error because the band gap calculations of semiconductors are known to have an error of at least 50 percent. [7]

Plotting the band structure requires knowledge of the high symmetry lines between the high symmetry points, the points used in a comparison plot will be Γ, M and K1 from

the Table 3.1 and Figure 3.2.

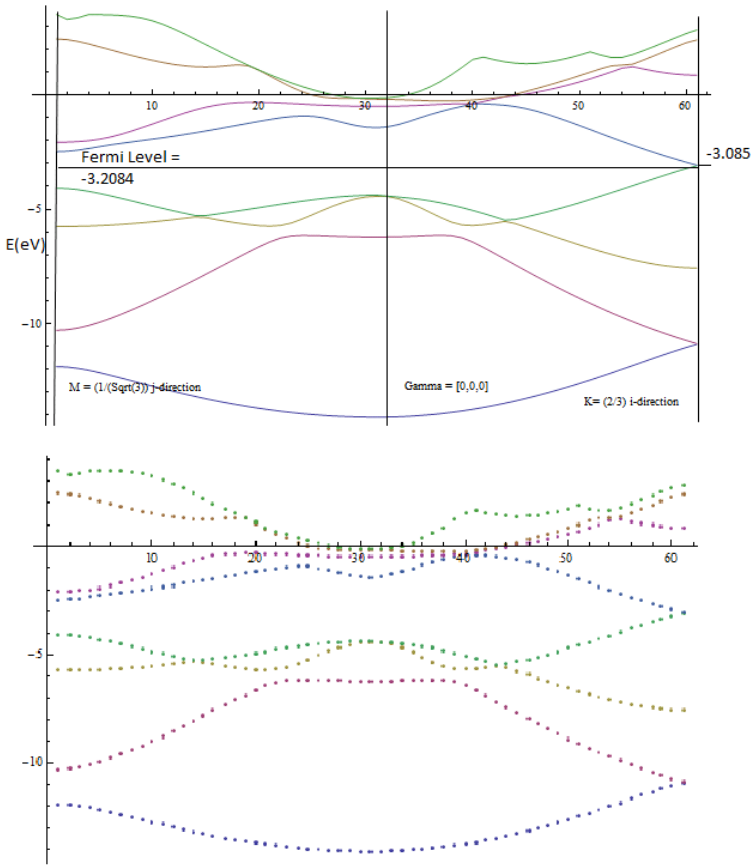

Figure 3.3: Quantum Espresso band structure plot of graphene

In order to verify the effectiveness of Quantum Espresso, the band structure needs to be compared to a well known accurate band structure model. See Figure 3.3 and how it compares to the correct band structure 3.4.

The graphing styles are slightly differenty but one can see that they are very similar. In the one calculated by Quantum Espresso, The lines do not appear to cross, but instead meet at points. This is just due to the graphical style of plotting.

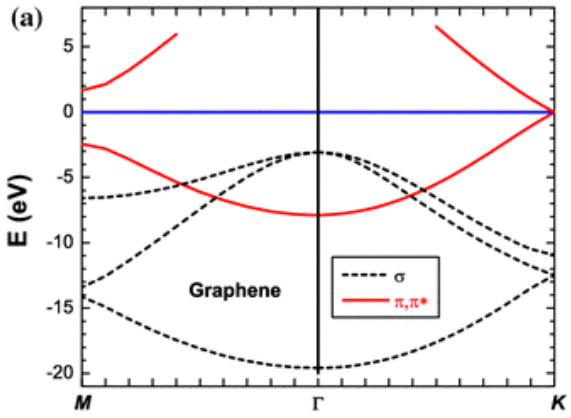

Figure 3.4: Band structure calculated in another paper [2]

New Research

4.1 New Research

The structure and unique characteristics of silicene and graphene have been shown, but the object of this thesis is to provide some new research towards integration and the practical use of these materials. To that effect a structure is proposed to combine them. The combination involves silicene placed upon graphene at the rate of one layer per layer of graphene. Superlattices may help to provide the bridge between the silicon based infrastructure and the unique properties of graphene. So multiple groups of bilayers of silicene and graphene will be considered as well. [14]

The physical compatibility of the two materials must first be taken into account. If one is to examine the lattice parameters of standard buckled silicene with respect to graphene you will notice that silicene upon graphene does not exhibit any long range symmetry. It may not seem immediately obvious, but since the atom to atom bond length of silicene is not a direct factor of the lattice parameter of graphene then it is essentially impossible to achieve the desired symmetry over the scope of this project. But as was mentioned before, materials placed in such proximity will exhibit an effect known as reconstruction. Reconstruction is the process where atoms at the boundaries in a solid reposition themselves to better accommodate the new material. This is especially important to consider in the case of a single layer, because the entirety of both layers will undergo reconstruction. However as the bilayers are allowed to relax, the software automatically takes this reconstruction

into consideration. If the single layers experiences reconstruction and reach an equilibrium state, it is not necessarily true that multiple layers will reach a similar equilibrium. So both a bilayer and superlattice structure calculations will be done to examine any differences. All calculations have a threshold convergence of $1 * 10^{-8}$ Rydbergs. For the the two-dimensional structures a 20 x 20 x 1 Monkhort- Pack mesh of k-points have been used. For three dimensional structures a 20 x 20 x 20 have been used. The cutoff energy has been set to 60 rydbergs. The functionals used are Perdew-Burke-Ernzerhof(PBE) GGA pseudopotentials. Generalized gradient approximations or GGA's are a type of functional that include spin as in the localized spin density, however the GGA's include gradients of the spin densities. The PBE-GGA uses the key characteristics of both the localized spin density functional or LSD as well as the GGA's major characteristics to calculate the psuedopotentials of the atoms. This methodology is better at dealing with density inhomogeneity than previous functionals. [38]

4.1.1 Bilayer Silicene and Graphene

Now that the goals and various types of bilayer and superlattice structures have been outlined there is another issue to address. There are two different types of unit cells that are possible to achieve long range symmetry in these structures. The first is the well known SiC_2 which has a silicon atom placed above the center of each hexagon in graphene. There is another structure not considered in previous research that retains more of the original structure of silicene. It has a unit cell composed of two silicons and six carbons and will be known as Si_2C_6. It has lower symmetry than the previously mentioned structure. In Figure 4.1 you can see a diagram of the unit cell of SiC_2 where the smaller atoms are the carbons and the larger ones are silicon. This ideal structural image is given so that it is possible to see what the structure might look like. This will be used as a model for the input, and then if there are any changes the output structure will be used for any further calculations. If the output structure reaches equilibrium near these initial conditions a secondary set of inputs

will be used to reverify the equilibrium structure. This is to make sure that a local minimum does not dominate the equilibrium structure. Several initial starting positions are used, not all are documented here. This methodology is used for all lattice structure determinations.

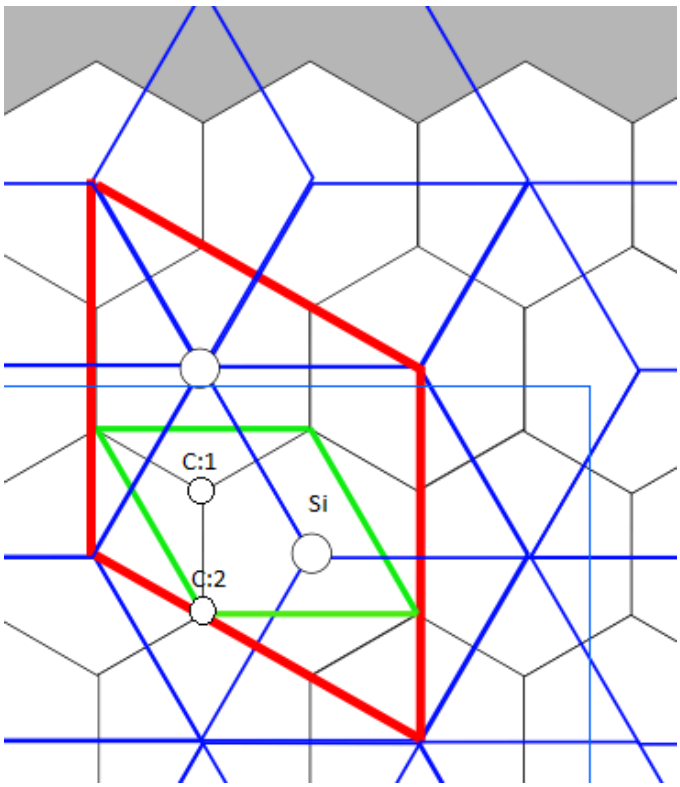

Figure 4.1: SiC_2

Which you can compare to the structure originally proposed. [2]

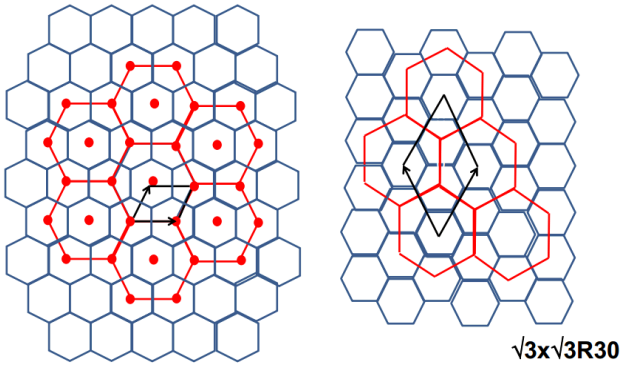

Figure 4.2: The originally proposed structure

Table 4.1 gives the coordinates of the atoms in the unit cell for the standard SiC_2 unit cell given in Figure 4.4.

Table 4.1: Atomic Coordinates: SiC_2

Atoms	x	y	z
C:1	0	0	0 $\mathring{A}$
C:2	0	1.42000 $\mathring{A}$	0 $\mathring{A}$
Si:1	1.225 $\mathring{A}$	0.71010 $\mathring{A}$	2

In Figure 4.1 you can see the ideal structure of SiC_2. As you can see, the silicon atoms reside above the carbon atoms, directly above the center of each hexagonal graphene structure. In Figure 4.3 you can see an image of what the input structure looks like after being plotted by the crystal plotting software. [39]

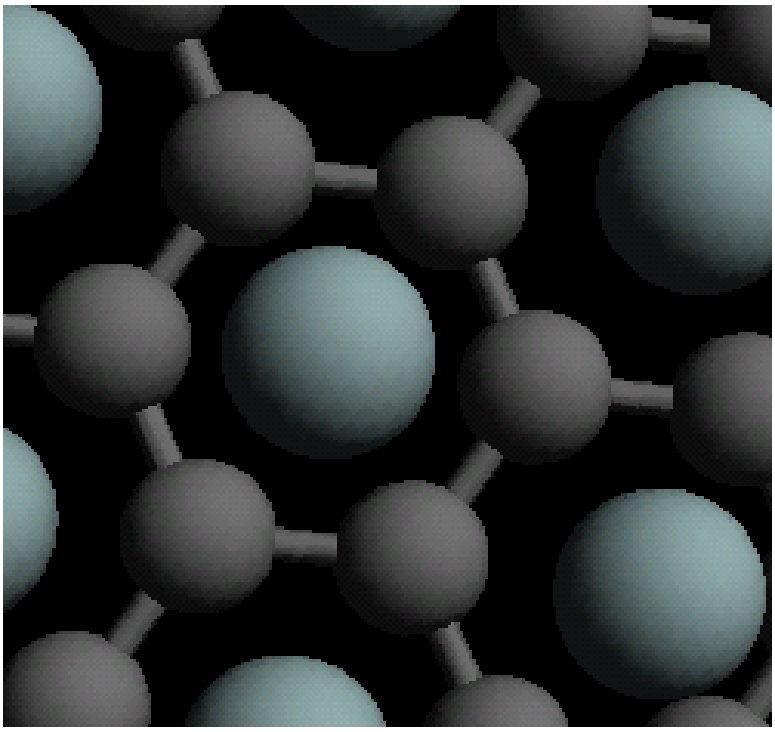

Figure 4.3: SiC_2, ideal structure image drawn with Avogadro software [39]

Upon structural relaxation with a cutoff energy of 60 Ry and a vacuum layer of 20 $\mathring{A}$, where the unit cell was both fixed and allowed to vary, the lowest energy structure given by Quantum Espresso is provided in Table 4.2 below. Similar to the background section, Various input positions and lattice parameters were considered. The below configuration is the minimum energy structure of those examined with the SiC_2 unit cell.

Table 4.2: Atomic Coordinates: SiC_2

Atoms	x	y	z
C:1	0	0	-0.767 $\mathring{A}$
C:2	0	1.42000 $\mathring{A}$	-0.767 $\mathring{A}$
Si:1	1.225 $\mathring{A}$	0.7110 $\mathring{A}$	3.505 $\mathring{A}$

Table 4.2 is a table of the positions of the atoms after they have been optimized. As

you can tell from the table of the output, the positions have changed little from the original position. It is worth mentioning that while this new position is a local minimum, there is another minimum located at another position, where the y-coordinate is $1.10\mathring{A}$ Keep in mind that the difference between these two minimums is on the order of 3^{-4} Rydbergs. Since they are so close in energy it is difficult to predict which configuration is more likely to occur in a laboratory situation. However the positions given in the table correspond to the lowest energy state found. In Figure 4.4 and 4.5 there are two visuals of the post-relaxation unit cell and and a visual of various angles of a bilayer slab respectively.

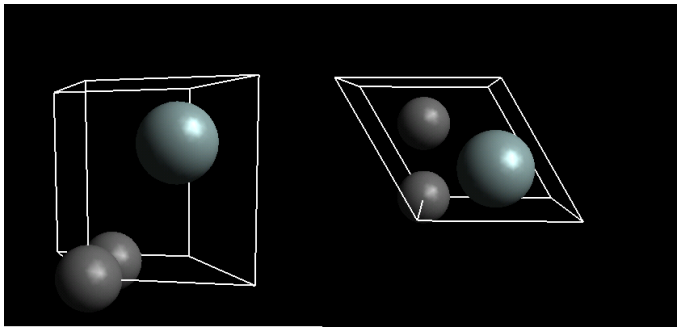

Figure 4.4: SiC_2, Unit cell drawn with the Avogadro software [39]

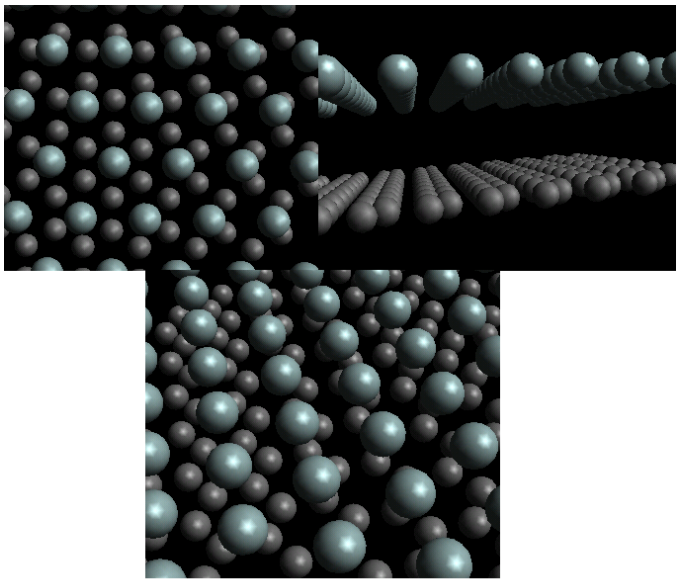

Figure 4.5: SiC_2, optimized structure of a bilayer slab drawn with the Avogadro software [39]

Now that the equilibrium lattice structure of a bilayer has been determined the band structure of the bilayer can be outlined. The band structures are calculated using an algorithm designed externally from Quantum Espresso plotting a minimum of 60 equally spaced points.

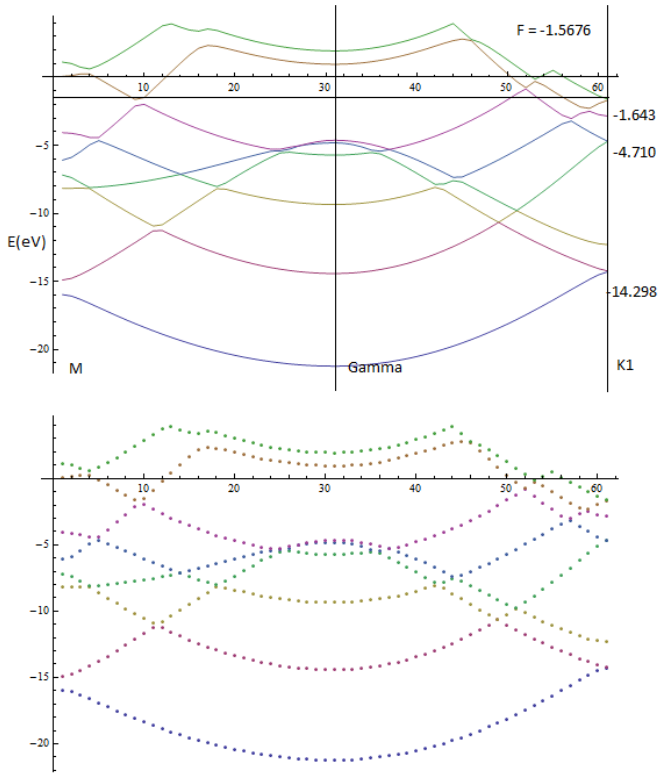

Figure 4.6: SiC_2, bilayer band structure

Both the individual points and a graphically smoothed version are given to avoid any confusion as to how the plotting program interprets the points. Below is the original band structure submitted in the paper by the Zhang et al. [2]

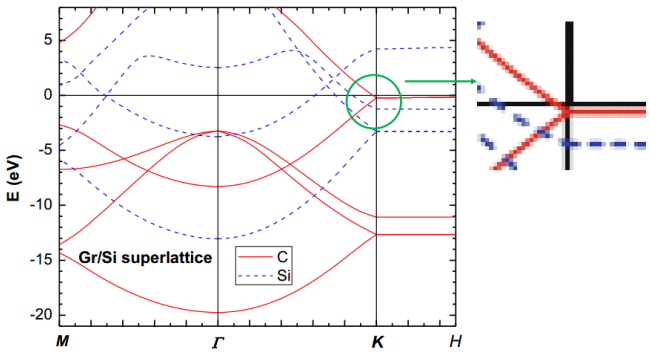

Figure 4.7: SiC_2, bilayer band structure comparison [2]

One can see upon cursory examination that the two structures are very similar. This helps to verify the methodology used here.

Now that the equilibrium structure of the first bilayer structure has been determined the next step is to analyze the other bilayer structure, Si_2C_6. It has more atoms per unit cell than the standard SiC_2. Figure 4.8 gives the structure of Si_2C_6 and you can see the coordinates of the various atoms in the Table 4.3. Also since the unit cell is larger a different lattice parameter is used to define the structure. It has been set to 4.24 $\mathring{A}$ so as to set the minimum bond length at 2.45 $\mathring{A}$. This is what allows the long range symmetry to work out. Once again these are the positions used for an initial input calculation.

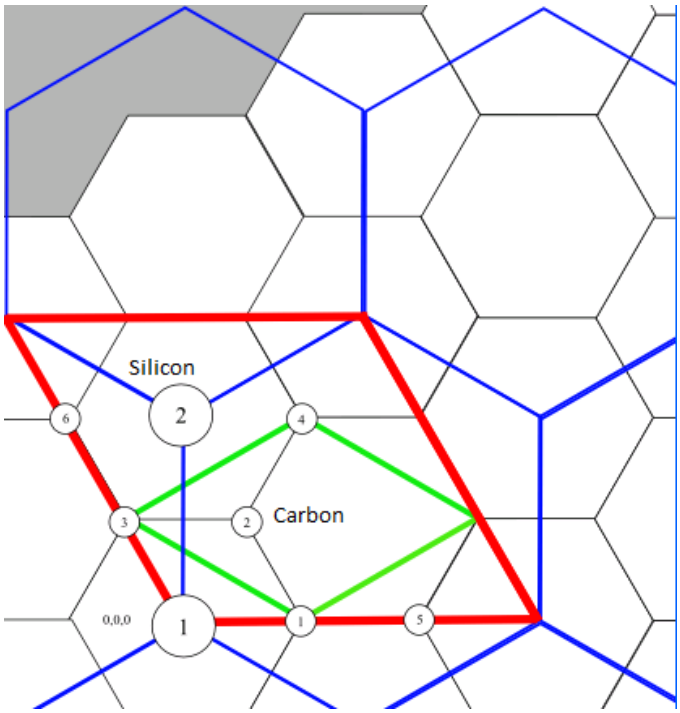

Figure 4.8: Si_2C_6

Table 4.3: Atomic Coordinates: Si_2C_6

Atoms	x	y	z
Si:1	0	0	2
Si:2	0	2.45 $\mathring{A}$	2
C:1	-0.71 $\mathring{A}$	1.225 $\mathring{A}$	0
C:2	-1.42 $\mathring{A}$	2.45 $\mathring{A}$	0
C:3	0.71 $\mathring{A}$	1.225 $\mathring{A}$	0
C:4	1.42 $\mathring{A}$	0	0
C:5	2.84 $\mathring{A}$	0	0
C:6	1.42 $\mathring{A}$	2.45 $\mathring{A}$	0

Table 4.3 gives the coordinates of the various atoms in the unit cell for Si_2C_6. The lower symmetry of the system requires more atoms per unit cell.

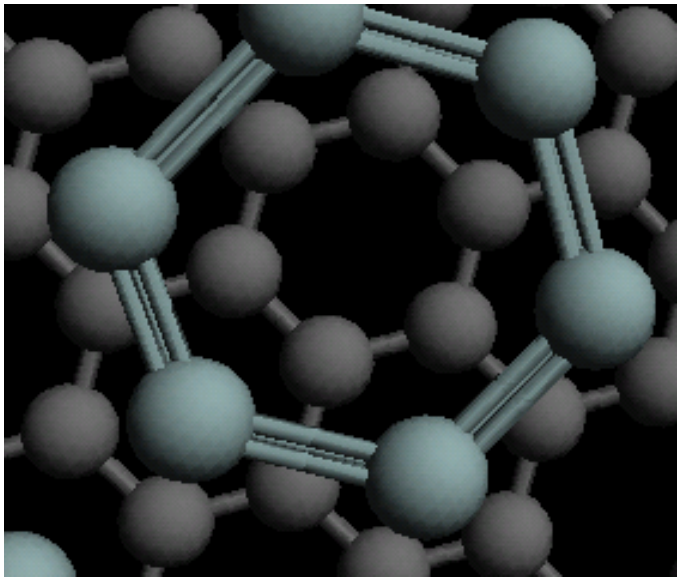

Figure 4.9: Si_2C_6, ideal structure drawn with Avogadro software [39]

Upon structural relaxation with a cutoff energy of 60 Ry and a vacuum layer of 20 $\mathring{A}$, where the unit cell was both fixed and allowed to vary, the lowest energy structure provided by Quantum Espresso is given in Table 4.4 below. Similar to the background section various input positions and lattice parameters were considered. The configuration outlined in Table 4.4 and Figure 4.10, is the minimum energy structure of those with the Si_2C_6 unit cell. Notice a significant deviation in positions of the atoms from the input to the output.

Table 4.4: Atomic Coordinates: Si_2C_6

Atoms	x	y	z
Si:1	0.0093 $\mathring{A}$	0	3.78$\mathring{A}$
Si:2	0.0101 $\mathring{A}$	2.449 $\mathring{A}$	3.80 $\mathring{A}$
C:1	-0.704 $\mathring{A}$	1.226 $\mathring{A}$	-0.59 $\mathring{A}$
C:2	-1.413 $\mathring{A}$	2.453 $\mathring{A}$	-0.59 $\mathring{A}$
C:3	0.713 $\mathring{A}$	1.226 $\mathring{A}$	-0.59 $\mathring{A}$
C:4	1.422 $\mathring{A}$	0.001 $\mathring{A}$	-0.59 $\mathring{A}$
C:5	2.840 $\mathring{A}$	0.001 $\mathring{A}$	-0.59 $\mathring{A}$
C:6	1.422 $\mathring{A}$	2.454 $\mathring{A}$	-0.59 $\mathring{A}$

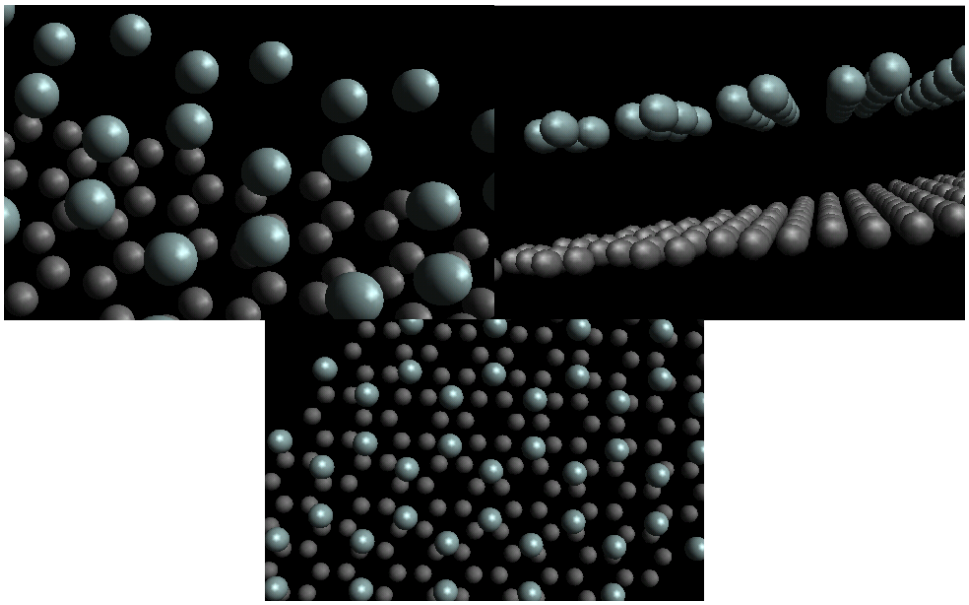

Figure 4.10: Si_2C_6, optimized structure drawn with Avogadro software [39]

The relaxation geometry has been outlined as before so the next step is to calculate the band structure of the new material. The band structure is,

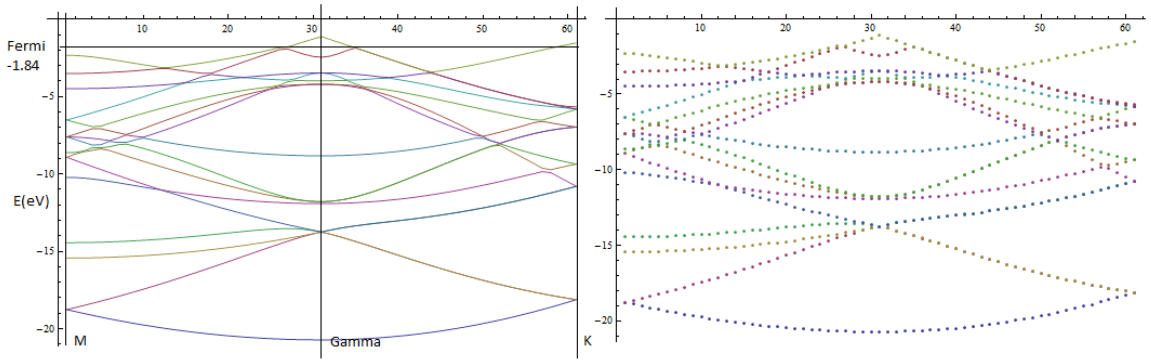

Figure 4.11: Si_2C_6, bilayer band structure

There is no comparison for this graph, apparently it has no previous counterpart.

Now that the two types of bilayers of silicene and graphene have been examined, the next step is to outline a different ways to arrange the silicene with respect to graphene. It

has been theorized that a superlattice will be the most stable system as well as the easiest to synthesize. Up until now the only structures that have been outlined are single bilayers. But a superlattice would contain multiple bilayers. Think of a superlattice as graphene with silicene used as a binding agents between the layers. [2]

4.1.2 Superlattice Calculations

The superlattice structure has the same basic unit cell as the unit cells of the two bilayer structures. The primary difference in the superlattice is that instead of a 20 $\mathring{A}$ vaccuum layer between bilayers, the bilayers are allowed to continue. The distance between the bilayers or, if one prefers, between layers is set. This is important as creating a single bilayer could be very difficult, but creating multiple bilayers should be easier to accomplish experimentally.

One would expect that a superlattice might have a different configuration of lowest energy with respect to the unit cell. Upon a relaxation the superlattice unit cell moves to the locations in the table below. There are some minor difference between the superlattice and the bilayer.

Table 4.5: Atomic Coordinates: SiC_2

Atoms	x	y	z
C:1	0	0.01229 $\mathring{A}$	-0.45507 $\mathring{A}$
C:2	0	1.41662 $\mathring{A}$	-0.418172 $\mathring{A}$
Si:1	1.234 $\mathring{A}$	0.7109 $\mathring{A}$	3.34907 $\mathring{A}$

Where the unit cell looks like,

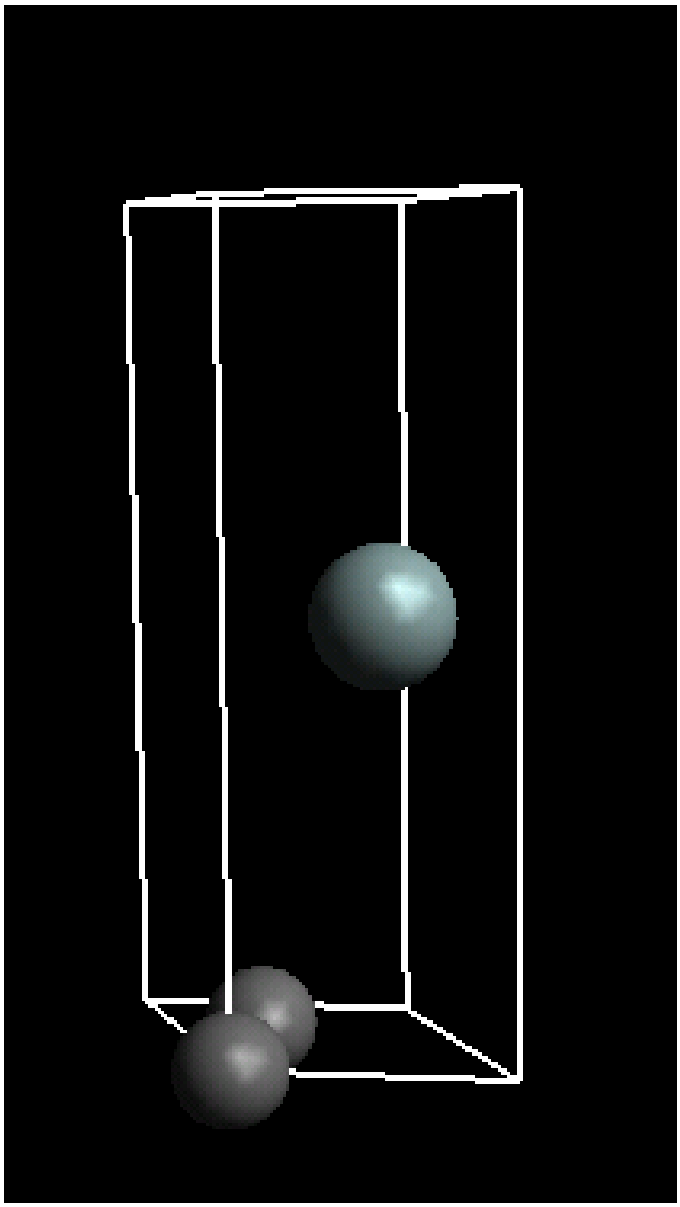

Figure 4.12: SiC_2, superlattice unit cell

and the superlattice structure looks like,

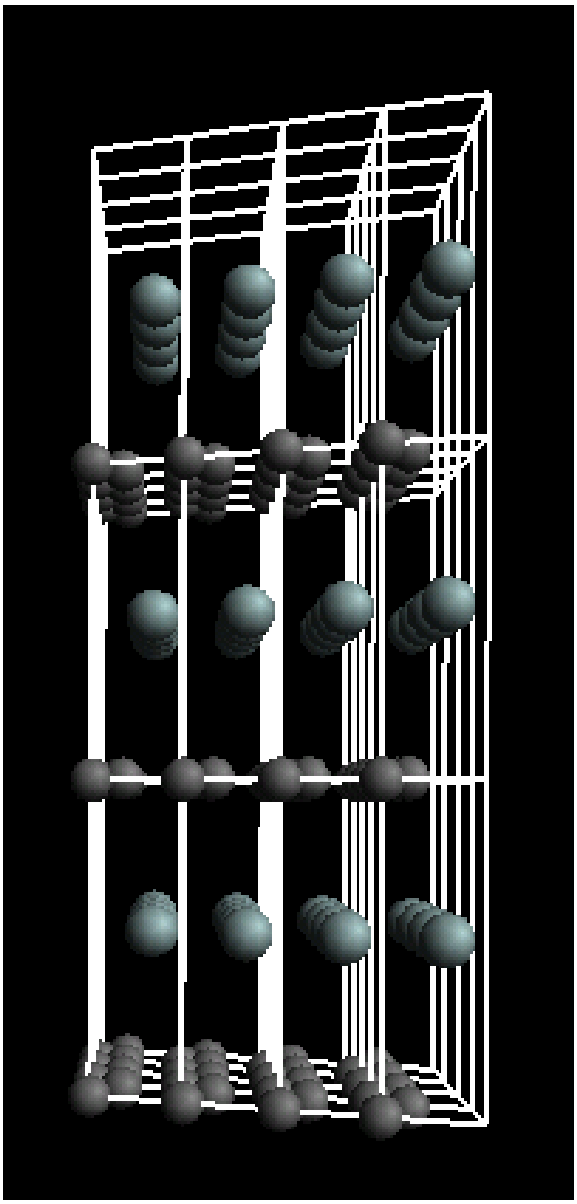

Figure 4.13: SiC_2, superlattice repeated in all 3 dimensions

Since the structure of the superlattice has been verified, one of the key goals of this paper can be examined. That goal is to show that this superlattice gives an increase of the binding energy over graphite. From the data on the superlattice the total energy comes to -30.635706 Ry, the energy of two-dimensional graphene minimizes at -22.795567 Ry and the results for buckled silicene are -7.84832809 Ry. When using the same formula that Zhang and his group used for the binding energy outlined in Section 2.11, a different value

is gained than what was reported. There are two unique layers in the superlattice and the sum of their individual energies are 0.00272969 Ry greater than the full superlattice energy.

$$\frac{(-30.635706 - (-22.795567 + -7.84832809)}{3} = 0.002729 \tag{4.1}$$

The value given is in Ry, but when one converts the value it gives 37.12 meV/atom which is reasonably close to the prior reported value of 35.1 meV/atom, which is larger than both of the two different forms of graphite which have reported values of 24.4 and 15.0 meV/atom. [2]

The binding energy energy has been examined which is dependent on the structural calculations, next the band structure calculations will be needed to examine the other primary goal of this paper, the shift in the Fermi level.

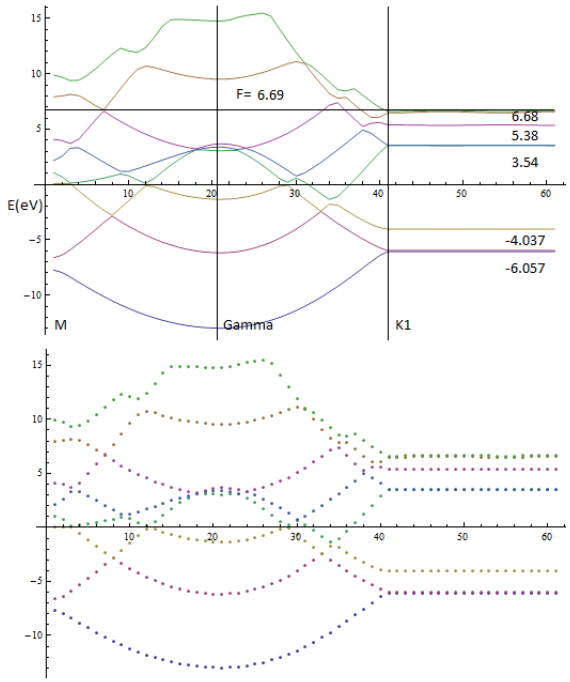

Figure 4.14: SiC_2, superlattice band structure

This band structure, Figure 4.14, runs through the same high symmetry points as Figure 4.6, except now it is plotted through the H point. Now the band structures will be

examined with regards to the goal of this paper.

The band structure calculations lead to a very similar answer as to that which is given by Doctor Zhang. You can see from Figure 4.14 that the difference between the Fermi energy and the nearest dirac point is 0.01 eV higher than the Fermi level. This is slightly less than what was predicted by Zhang et al. If you look at the bilayer structure of the bilayer SiC_2 then you have results that agree more closely. The nearest dirac point to the Fermi level in the bilayer band structure diagram is 0.0754 electron volts below the Fermi level. This value is closer to the reported value of 0.245 eV. In this case, the shift of the Fermi level above dirac points may represent a charge transfer from the silicon in the lattice to the graphene. The increase in the Fermi level can causethe superlattice to have increased electron transport over standard graphene. Both values of the change in the Fermi level in the band structures agree with the trend of the increase of the Fermi level. With respect to the value of the increase it appears that the methodology used here appears to underestimate this value as the ones documented are much lower than the accepted.

Earlier two different kinds of bilayer structures were examined. Here the second superlattice Si_2C_6 will be examined in the same manner that SiC_2 has been. Upon optimization the location of the atoms move to the positions in Table 4.6.

Table 4.6: Atomic Coordinates: Si_2C_6

Atoms	x	y	z
Si:1	0.4825 $\mathring{A}$	0.286 $\mathring{A}$	3.511$\mathring{A}$
Si:2	0.48922 $\mathring{A}$	2.704 $\mathring{A}$	4.133 $\mathring{A}$
C:1	-0.7448 $\mathring{A}$	1.219 $\mathring{A}$	-0.157 $\mathring{A}$
C:2	-1.228 $\mathring{A}$	2.024 $\mathring{A}$	-1.064 $\mathring{A}$
C:3	0.7598 $\mathring{A}$	1.214 $\mathring{A}$	-0.764 $\mathring{A}$
C:4	1.5066 $\mathring{A}$	-0.147 $\mathring{A}$	-1.380 $\mathring{A}$
C:5	2.981 $\mathring{A}$	-0.019$\mathring{A}$	0.168 $\mathring{A}$
C:6	0.992 $\mathring{A}$	2.516 $\mathring{A}$	-0.447 $\mathring{A}$

One can see from Table 4.6 that this superlattice form is highly irregular. If it is deemed worthwhile, this second structure may need to be proven unstable experimentally. However because of the breakdown of the hexagonal graphene like structure that gives rise to the unique Dirac points this structure will no longer be examined. All of the structural data has now been presented.

4.2 Conclusions

Now all the simulated data has all been presented, it must be analyzed. Since Quantum Espresso has shown reasonable accuracy in providing electronic and structural results in similar cases, it is reasonable to assume that the results it has given are trustworthy. The band structure diagram of graphene was nearly identical to a previous accepted diagram. This is further verification of the methodology.

With that being said, the results that have been obtained also match to a certain de-

gree the results of another researcher in the field. Doctor Zhang and his associates have also calculated the superlattice electronic and lattice structures for SiC_2. This thesis has set out verify this research as well as possibly expand on a different superlattice structure. The Si_2C_6 was proposed theoretically in a presentation given by Zhang, but was not examined in depth. Here the unit cell and basic structure have been outlined and the results of the equilibrium structure have been obtained. Upon examination, the new structure, Si_2C_6, does not appear to be worth further consideration. The structure loses the hexagonal structure that creates the unique properties of graphene as the band structure and transport properties are almost entirely dependent on structure.

Improved binding energy and enhanced transport properties are the proposed benefits of the original superlattice structure with silicene as the intercalate. This paper has also shown these proposed benefits, but not to the same degree as Doctor Zhang. His results are considered reliable, so that means the methodology in this paper underestimates both the shift in the Fermi energy and the Binding energy. The binding energy calculated by Doctor Zhang is 35.1 meV/atom, whereas here it is calculated to be 37.12 meV/atom. The Fermi level is predicted to be 234 meV above the Dirac point, where in this paper the Fermi level is only 10 meV above. This means there is some sort of systematic error in this methodology for the graphing of the Dirac points. The new type of functional was reported to be better at estimating band structure calculations. However, it appears to have done an acceptable job of calculating the binding energy, but it apparently failed at the graphing of the Dirac point. This could be some sort of error in the methodology and it is possible that changing the input values may yield a similar value.

In conclusion, the structure of the superlattice has been verified to be the same as what was predicted in the paper by Zhang. [2] In this case the open source software, Quantum Espresso, was used as well as a different type of functional. Because of the different functional, some variation in the band structure is to be expected. The positions of the Dirac points maintain the same pattern that was predicted, which leads to silicon providing extra

charge for graphene and the binding energy does indeed increase over graphite. So the results here do not completely agree with the accepted values, but they do help to show the continued usefulness of the superlattice structure, if only for a way to utilize the Dirac points in practical applications.

Appendix A

5.1 Plane Wave-Self Consistent Calculations

This section defines how to run a basic plane wave calculation in Self Consistent mode to find charge density. The first thing that needs to be done is define an input file. The previous section has covered how to write the input file. This section will show how to run the file. Keep in mind that all the programs are in bin directory inside the Quantum Espresso Directory, so that is where one needs to direct the command line to find them.

```
(Bin Directory) = ~/espresso-4.3.2/bin/pw.x

prompt> ~bin/pw.x < Name of input > Name of output
```

This is all that is needed, as long as the input file is written properly. In the above example the name of the input is not arbitrary, but the name of the output is arbitrary. Input is based on the name inside the file. e.g. si.scf.in, whereas the output file can have any name that you want. Keep in mind that this will create a temporary file as well to work with, so two new files will be created in the directory.

The key here is to remember that the program is running an algorithm that uses a numerical process to implement the physics that was mentioned in the theory section. This charge density algorithm that is mentioned here is finding wavefunctions that fit the given input. This input that is being used is designated as self-consistent field calculation. There

are various other types of calculations that can be specified from the input file. They are outlined below.

- Self-Consistent Field Calculation ('scf')

A self-consistent field calculation uses a plane wave pseudopotential method to determine the Kohn Sham wavefunctions and their solutions. It does so using an algorithm called the modified broyden method. [40] Every time the plane wave algorithm is called, it begins by using this broyden method. It is the foundation of the rest of the calculations in Quantum Espresso. Once the kohn-sham wavefunctions have been determined we can use them to determine the charge density. From basic quantum mechanics it is known that it is calculated by summing over the modulus of the wavefunctions squared.

- Non Self Consistent Field Calculation ('nscf')

This calculation always has to follow a self-consistent field calculation. Once the orbitals are determined one can use this method to determine the density of states.

- Band Structure Calculation ('bands')

This calculation always has to follow a self-consistent field calculation. Once again the orbitals need to be determined and by a standard Brillouin zone sampling it will determine the band structure. Brillouin zone sampling, in this case, is a standard computational methods term that refers to the integration calculations that are done on the Brillouin zone to determine the properties of a solid.

5.2 Structural Optimization Methods

- Geometric Relaxation ('relax')

The relax method is used to calculate the relaxation positions of atoms in molecules or crystals. Like most of the molecular dynamics methods it uses the Broyden-Fletcher-Goldfarb-Shanno algorithm or BFGS for short. The relax method determines the equilibrium position of the atoms in a structure using geometry energy calculations. This relax method, unlike molecular dynamics, cannot conduct calculations at different temperatures. This method also maintains the unit cell parameters and can only shift the atoms while maintaining the periodicity.

- Molecular Dynamics ('md')

The molecular dynamics method is also used to determine the positions but it can calculate them at different temperatures. It uses the Verlet Algorithm to accomplish this task alongside the original BFGS. It has the same restrictions on cell parameters as the relax method.

- Variable Cell Molecular Dynamics ('vc-md')

This is essentially the same as the original molecular dynamics method except that the unit cell parameter is allowed to vary in this method.

- Variable Cell Geometric Relaxation ('vc-relax')

This is essentially the same as the original relaxation dynamics except that the unit cell is allowed to vary in this method. This version of the variable cell method uses the RM Wenzcovitch algorithm in conjunction with the BFGS.

5.3 Running Band Structure Calculation:

How to run a standard plane wave calculation, make sure that you include the 'bands' field in the CONTROL card.

```
prompt> ~/espresso-4.3.2/bin/pw.x < Input > Output
```

In this case we will use $si.band.in$ and $si.band.out$. You will need to delete the temporary file for this to work. Next you will need another band file to work with $si.bands.in$ However this file is basically used to create the right directory file, from the previous bands file.

```
prompt> ~/espress-4.3.2/bin/bands.x <  Input > Output
```

Use $si.bands.in$ and $si.bands.out$. It is sequential; you cannot use $si.bands.in$ unless you run $pw.x$ previously. Keep in mind it is also important to run the self consistent calculation before you run the band structure calculation Then you can run $plotband.x$ as

```
prompt> ~/espress-4.3.2/bin/plotbands.x
```

And then it asks for an input. You have to choose a range for the energies, so pick lower than the lowest. In this case choose -6. Here we will choose 10 just as an example. It does not graph the entire range of the band structure. To do that you will simply choose higher than the highest energy value. Choose two different file names for outputs, like in previous examples. Then choose a guess at a Fermi energy. Let us choose 6.337 for this example. It will then ask for a range of energies, the change in energy (delta energy) and a reference energy. Choose the Fermi energy as a reference and then choose 1 for the delta energy. If you choose the wrong Fermi energy, the band structure comes out incorrectly.

This methodology may work better in the newer version, but in the version 4.3.2 this process didn't work. So a program was written in Mathematica 7.0 to accomplish this task. [41]

5.4 Post Processing

Once you have run the plane wave you will need to take care of the post processing of the file. Post processing just means to take the file and extract the date from it so that it can be

run by the output plotting algorithm. The following file changes the plane wave file so that it is,

```
si.pp_rho.i

&inputpp

prefix = 'si'

outdir = '/home/w003pbb/tmp/'

filplot = 'sicharge'

plot_num= 0 // This tells it to be a charge plot

/

&plot

nfile = 1

// Number of data files

filepp(1) = 'sicharge'

// name of the file output

weight(1) = 1.0

 // Just like it says, it is a weighting factor

iflag = 2

// dimensions of plot, 2d plot.

output_format = 2

// Gives output type

fileout = 'si.rho.dat'

// name of the file

e1(1) =1.0, e1(2)=1.0, e1(3) = 0.0,

// 3d vectors that do the plotting lines

e2(1) =0.0, e2(2)=0.0, e2(3) = 1.0,
```

```
// for an input variable of iflag, the variables e2 are needed
nx=56, ny=40 // number of points in the plane
/
```

Then you just need to run the pp.x algorithm to garner the plotting files that we need.

```
prompt> ~/espress-4.3.2/bin/pp.x < Input > Output
```

Then it will generate two files based on the inputs. In the above case it provided a sicharge file and $si.rho.dat$. We don't need sicharge for now, but we do want the $.dat$ file. Now to generate the charge plot diagram you need to run another algorithm.

```
prompt> ~/espresso-4.3.2/bin/plotrho.x
```

And then give it the name of a file. In this case use $si.rho.dat$. It will ask for a name. Give it any name, in this case use $si.rho.ps$. It will also ask for a logarithmic scale, tell it 'no' for now. Then it will ask you to choose a scale. Choose one greater than both the bounds it gives you and make the maximum number of levels 6. This is just arbitrary for now.

5.5 Plotting Algorithm

Based on the .dat file created by Quantum Espresso, an algorithm was developed to plot it properly. For various reasons the plotting algorithm included in the Quantum Espresso package was unsuitable. Mostly due to the nature of the environment that the software was installed on. The algorithm has been included here for completeness.

```
File1 = Import["newbands.dat", "Table"];
(* This imports the file that we want *)
```

```
n = Dimensions[File1];
(* Takes in the dimensions of the .dat file that we imported. This \
only gives us the depth, or at least it should*)
x = n[[1]];
Iter = Table[2 i + 1, {i, 1, x/2}];
(* Here i'm iterating through the .dat file input to find the data \
that I want *)

Temp = Table[File1[[Iter[[i]]]], {i, x/2}];
(*  This fills the Funct matrix with other the data that we wanted, \
which are the energy levels of the bands *)
File1[[Iter[[1]], 1]];
Temp = Table[
   Something =
    Table[n*(File1[[Iter[[n]], i]]/n)^z, {i, 8}, {z, 0, 1}], {n, 1,
    x/2}];
(* This is an interesting bit,First File1[[Iter[[n]],i]] gives the \
components of the input matrix and then you need the z-value to give \
a 1 as the other part of the data point. Then then n variable when \
multiplies that 1 by the number you are on as well as iterate through \
the various rows of the data that we want. *)
```

```
Final = Table[Temp[[All, n]], {n, 1, 8}];


(* This bit reorients it so the matrix can be plotted properly *)
ListLinePlot[Final, Method -> None]
ListPlot[Final]
```

Bibliography

[1] Gian G. Guzmán-Verri and L. C. Lew Yan Voon. Electronic structure of silicon-based nanostructures. *Physical Review B (Condensed Matter and Materials Physics)*, 76(7):075131, 2007.

[2] Yong Zhang and Raphael Tsu. Binding graphene sheets together using silicon: Graphene/Silicon superlattice. *Nanoscale Research Letters*, February 2010.

[3] A. K. Geim and K. S. Novoselov. The rise of graphene. *Nature Materials*, 6(3):183–191, 2007.

[4] S. Cahangirov, M. Topsakal, E. Aktürk, H. Şahin, and S. Ciraci. Two- and one-dimensional honeycomb structures of silicon and germanium. *Physical Review Letters*, 102(23):236804, 2009.

[5] YuChen Wang, Kurt Scheerschmidt, and Ulrich Gösele. Theoretical investigations of bond properties in graphite and graphitic silicon. *Phys. Rev. B*, 61(19):12864–12870, May 2000.

[6] Zeyuan Ni, Qihang Liu, Kechao Tang, Jiaxin Zheng, Jing Zhou, Rui Qin, Zhengxiang Gao, Dapeng Yu, and Jing Lu. Tunable bandgap in silicene and germanene. *Nano Letters*, 12(1):113–118, 2012.

[7] P. Mori-Sánchez, A. J. Cohen, and W. Yang. Localization and Delocalization Errors in Density Functional Theory and Implications for Band-Gap Prediction. *Physical Review Letters*, 100(14):146401, April 2008.

[8] Ilker Demiroglu, Daniele Stradi, Francesc Illas, and Stefan T Bromley. A theoretical study of a zno graphene analogue: adsorption on ag(111) and hydrogen transport. 23(31):334215–334215, 2011.

[9] A.J. Lu, X.B. Yang, and R.Q. Zhang. Electronic and optical properties of single-layered silicon sheets. *Solid State Commun.*, 149(2):153–155, 2009.

[10] M. Houssa, G. Pourtois, V. V. Afanasev, and A. Stesmans. Electronic properties of two-dimensional hexagonal germanium. 96:082111, 2010.

[11] M. Houssa, G. Pourtois, V. V. Afanasev, and A. Stesmans. Can silicon behave like graphene? a first-principles study. 97:112106, 2010.

[12] M. Houssa, E. Scalise, K. Sankaran, G. Pourtois, V. V. Afanasev, and A. Stesmans. Electronic properties of hydrogenated silicene and germanene. 98(22):223107, 2011.

[13] Xin-Quan Wang, Han-Dong Li, and Jian-Tao Wang. Induced ferromagnetism in one-side semihydrogenated silicene and germanene. *Phys. Chem. Chem. Phys.*, pages –, 2012.

[14] Jing Zhang, Jian-Min Zhang, and Ke-Wei Xu. First-principles study on structural and electronic properties of alnsix heterosheet. *Physica B: Condensed Matter*, 407(12):2301 – 2305, 2012.

[15] Yi Ding and Jun Ni. Electronic structures of silicon nanoribbons. *Applied Physics Letters*, 95(8):083115, 2009.

[16] Yi Ding and Yanli Wang. Electronic structures of silicene fluoride and hydride. *Applied Physics Letters*, 100(8):083102, 2012.

[17] E. Aktürk, C. Ataca, and S. Ciraci. Effects of silicon and germanium adsorbed on graphene. 96(12):23112, 2010.

[18] Shaoqing Wang. A comparative first-principles study of orbital hybridization in two-dimensional c, si, and ge. *Physical Chemistry Chemical Physics*, 13(25):11929–11938, 2011.

[19] N. D. Drummond, V. Zólyomi, and V. I. Fal'ko. Electrically tunable band gap in silicene. *Phys. Rev. B*, 85:075423, Feb 2012.

[20] O. Pulci, P. Gori, M. Marsili, V. Garbuio, A. P. Seitsonen, F. Bechstedt, A. Cricenti, and R. Del Sole. Electronic and optical properties of group iv two-dimensional materials. *Phys. Status Solidi A*, 207(2):291–299, 2010.

[21] Nelson Y Dzade, Kingsley O Obodo, Sampson K Adjokatse, Akosa C Ashu, Emmanuel Amankwah, Clement D Atiso, Abdulhakeem A Bello, Emmanuel Igumbor, Stany B Nzabarinda, Joshua T Obodo, Anthony O Ogbuu, Olu Emmanuel Femi, Josephine O Udeigwe, and Umesh V Waghmare. Silicene and transition metal based materials: prediction of a two-dimensional piezomagnet. 22:375502, 2010.

[22] Paola De Padova, Claudio Quaresima, Bruno Olivieri, Paolo Perfetti, and Guy Le Lay. sp2-like hybridization of silicon valence orbitals in silicene nanoribbons. 98(8):081909, 2011.

[23] G. Le Lay, B. Aufray, C. Léandri, H. Oughaddou, J.-P. Biberian, P. De Padova, M.E. Dávila, B. Ealet, and A. Kara. Physics and chemistry of silicene nano-ribbons. *Applied Surface Science*, 256(2):524–529, 2009.

[24] Hirotaka Okamoto, Yusuke Sugiyama, and Hideyuki Nakano. Synthesis and modification of silicon nanosheets and other silicon nanomaterials. *Chemistry*, 17(36):9864–9887, 2011.

[25] Boubekeur Lalmi, Hamid Oughaddou, Hanna Enriquez, Abdelkader Kara, Sébastien Vizzini, Bénidicte Ealet, and Bernard Aufray. Epitaxial growth of a silicene sheet. 97(22):223109, 2010.

[26] B. Feng, Z. Ding, S. Meng, Y. Yao, X. He, P. Cheng, L. Chen, and K. Wu. Evidence of silicene in honeycomb structures of silicon on Ag(111). *eprint arXiv:1203.2745*, March 2012.

[27] A. Kara, C. Léandri, M. E. Dávila, P. de Padova, B. Ealet, H. Oughaddou, B. Aufray, and G. Le Lay. Physics of silicene stripes. *Journal of Superconductivity and Novel Magnetism*, 22:259, 2009.

[28] P. Zhang, X.D. Li, C.H. Hu, S.Q. Wu, and Z.Z. Zhu. First-principles studies of the hydrogenation effects in silicene sheets. *Physics Letters A*, 376(14):1230 – 1233, 2012.

[29] G G Guzmn-Verri and L C Lew Yan Voon. Band structure of hydrogenated si nanosheets and nanotubes. *Journal of Physics: Condensed Matter*, 23(14):145502, 2011.

[30] Deepthi Jose and Ayan Datta. Structures and electronic properties of silicene clusters: a promising material for fet and hydrogen storage. *Phys. Chem. Chem. Phys.*, 2011.

[31] S. Cahangirov, C. Ataca, M. Topsakal, H. Sahin, and S. Ciraci. Frictional figures of merit for single layered nanostructures. *Phys. Rev. Lett.*, 108:126103, Mar 2012.

[32] Tetsuya Morishita, Michelle J.S. Spencer, Salvy P. Russo, Ian K. Snook, and Masuhiro Mikami. Surface reconstruction of ultrathin silicon nanosheets. *Chemical Physics Letters*, 506(4-6):221 – 225, 2011.

[33] D. Sholl and J.A. Steckel. *Density Functional Theory: A Practical Introduction*. John Wiley & Sons, Incorporated, 2011.

[34] J. Patterson and B. Bailey. *Solid-State Physics: Introduction to the Theory*. Springer, 2011.

[35] Lok C. Lew Yan Voon, 2012. Private Lectures.

[36] Yunkai Zhou Yousef Saad James R. Chelikowsky Tzu-Liang Chan, Murilo L. Tiago. Efficient algorithms for the electronic structure of nanocrystals, 2008. $http : //www.mcc.uiuc.edu/workshops/electronicstructure/2008/talks/04_Chan_T.pdf$.

[37] Hui Zhang, Jin-Ho Choi, Yang Xu, Xiuxia Wang, Xiaofang Zhai, Bing Wang, Changgan Zeng, Jun-Hyung Cho, Zhenyu Zhang, and J. G. Hou. Atomic structure, energetics, and dynamics of topological solitons in indium chains on si(111) surfaces. *Phys. Rev. Lett.*, 106(2):026801, Jan 2011.

[38] John P. Perdew, Kieron Burke, and Matthias Ernzerhof. Generalized gradient approximation made simple. *Phys. Rev. Lett.*, 77(18):3865–3868, October 1996.

[39] Avogadro: an open-source molecular builder and visualization tool. version 1.03. http://avogadro.openmolecules.net/.

[40] Paolo Giannozzi, Stefano Baroni, Nicola Bonini, Matteo Calandra, Roberto Car, Carlo Cavazzoni, Davide Ceresoli, Guido L Chiarotti, Matteo Cococcioni, Ismaila Dabo, Andrea Dal Corso, Stefano de Gironcoli, Stefano Fabris, Guido Fratesi, Ralph Gebauer, Uwe Gerstmann, Christos Gougoussis, Anton Kokalj, Michele Lazzeri, Layla Martin-Samos, Nicola Marzari, Francesco Mauri, Riccardo Mazzarello, Stefano Paolini, Alfredo Pasquarello, Lorenzo Paulatto, Carlo Sbraccia, Sandro Scandolo, Gabriele Sclauzero, Ari P Seitsonen, Alexander Smogunov, Paolo Umari, and Renata M Wentzcovitch. Quantum espresso: a modular and open-source software project for quantum simulations of materials. *Journal of Physics: Condensed Matter*, 21(39):395502 (19pp), 2009.

[41] Inc. Wolfram Research. Mathematica edition: Version 7.0, 2008. Champaign, Illinois.